

**COMPARISON OF LAMINAR AND TURBULENT MODEL OF WATER FLOW
IN MICROCHANNEL**

MOHAMED FIQRI BIN AHMED FAUZI



Faculty of Mechanical Engineering

UNIVERSITI TEKNIKAL MALAYSIA MELAKA

2018

DECLARATION

I declare that this thesis entitled “Comparison of Laminar and Turbulent Model of Water Flow in Microchannel” is the result of my own research except as cited in the references. The thesis has not been accepted for any degree and is not concurrently submitted in candidature of any other degree.



Signature :.....
اونيورسي تيكنيكل مليسيا ملاك

Name of Supervisor :.....
UNIVERSITI TEKNIKAL MALAYSIA MELAKA

Date :.....

APPROVAL

I hereby declare that I have read this project report and in my opinion this report is sufficient in terms of scope and quality for the award of the degree of Bachelor of Mechanical Engineering (Hons).



Signature :

Name of Supervisor : Dr. Ernie Binti Mat Tokit

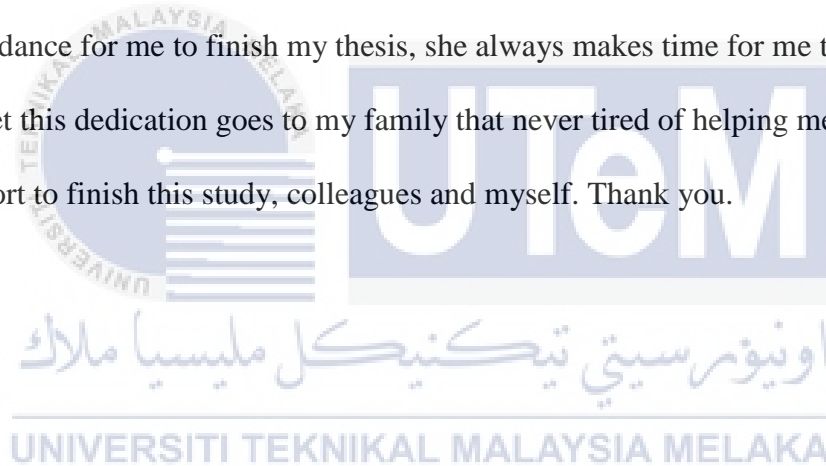
Date :

اونيورسيتي تيكنيكل مليسيا ملاك

UNIVERSITI TEKNIKAL MALAYSIA MELAKA

DEDICATION

This thesis is dedicated for the sake of Allah, my Creator and my Master, my great teacher and messenger, Muhammad (May Allah bless and grant him), who taught us the purpose of life. Other than that, this thesis is dedicated to Dr. Ernie Binti Mat Tokit how is always give me guidance for me to finish my thesis, she always makes time for me to educate me. Not to forget this dedication goes to my family that never tired of helping me and give me moral support to finish this study, colleagues and myself. Thank you.



ABSTRACT

A flow can be laminar, turbulent or transitional in nature. This become a very important classification of flow. Laminar and turbulent flow can be test to get the different of the result. The objective of this study are to find temperature distribution, mesh independent test, entrance length and find Nusselt number and the different between laminar and turbulent flow. Temperature distribution can be conduct with running the simulation that the domain have been create using software. Software that have been using in this experiment to draw the domain is GAMBIT software and that was one of the method in this study. The simulation need to consider the material use and boundary condition. Then run the simulation with iterate is set to 1000 and when the worlds converge appear the simulation will stop and the running of simulation is done. To make the simulation is valid, the numerical code is verified by contrasting or comparing it with available analytical solution or widely accepted numerical results. The largest deviation between simulation result from Qu and Mudawar result is 13.1%. The simulation is considered as valid since the simulation is showing the identical pattern. Temperature distribution can be seen in the contour where the temperature at the inlet, middle and outlet is different. The finding shows that temperature for the laminar and turbulent flow is different. Analyses data showed that turbulent flow temperature is higher than laminar. The range of hydraulic diameter are between 8.658×10^{-5} to 2.52×10^{-5} . Average range for Nusselt number in this project is between 4 to 40 Nusselt numbers. Turbulent method was using k-epsilon in simulation.

UNIVERSITI TEKNIKAL MALAYSIA MELAKA

ABSTRAK

Aliran boleh bersifat laminar, bergolak atau transisi. Ini menjadi klasifikasi aliran yang sangat penting. Laminar dan aliran bergelora boleh diuji untuk mendapatkan hasil yang berbeza. Objektif kajian ini adalah untuk mencari pengagihan suhu, uji bebas ujian, panjang pintu masuk dan mencari nombor Nusselt dan perbezaan antara aliran laminar dan turbulen. Pengedaran suhu boleh dijalankan dengan menjalankan simulasi yang domain telah dibuat menggunakan perisian. Perisian yang telah menggunakan dalam eksperimen ini untuk menarik domain adalah perisian GAMBIT dan itu adalah salah satu kaedah dalam kajian ini. Simulasi perlu mempertimbangkan penggunaan bahan dan syarat sempadan. Kemudian jalankan simulasi dengan iterate ditetapkan ke 1000 dan apabila dunia menumpu muncul simulasi akan berhenti dan menjalankan simulasi dilakukan. Untuk membuat simulasi itu sah, kod berangka diverifikasi dengan membezakan atau membandingkannya dengan penyelesaian analisis yang tersedia atau keputusan berangka yang diterima secara meluas. Penyimpangan terbesar antara keputusan simulasi dari Q_u dan Mudawar ialah 13.1%. Simulasi dianggap sebagai sah kerana simulasi menunjukkan corak yang sama. Pengagihan suhu boleh dilihat dalam kontur di mana suhu di salur, tengah dan salur adalah berbeza. Hasilnya menunjukkan bahawa suhu bagi laminar dan aliran bergelora adalah berbeza. Analisis data menunjukkan suhu aliran turbulen lebih tinggi daripada laminar. Julat diameter hidraulik adalah antara 8.658×10^{-5} hingga 2.52×10^{-5} . Julat purata bagi nombor Nusselt dalam projek ini adalah antara 4 hingga 40 nombor Nusselt. Kaedah gelora menggunakan k -epsilon dalam simulasi.

ACKNOWLEDGEMENT

First and foremost, I would like to express my praise to Allah S.W.T for giving me the opportunity and strength to finish my final year project successfully. I would like to convey my gratitude to my supervisor, Dr Ernie Binti Mat Tokit for his guidance, encouragement and support along the way the project has taken place. He helped me a lot and giving me the space to grow myself independently.

I also would like to thank to my parents who always helped with moral support and in financial support for me to finish my task. .Not forgotten, I would like to thank to Mechanical Engineering Faculty of Universiti Teknikal Malaysia Melaka (UTeM) for providing a good facility to complete my project.

Last but not least, a huge thank to my colleagues who helped me through up and down and also my family for their words of encouragement that keeping me focus on completing this project.



CONTENT

| CHAPTER | CONTENT | PAGE |
|------------------|------------------------------------|------|
| | DECLARATION | ii |
| | ABSTRACT | iii |
| | ABSTRAK | iv |
| | ACKNOWLEDGEMENT | v |
| | TABLE OF CONTENT | vi |
| | LIST OF FIGURES | viii |
| | LIST OF TABLE | x |
| | LIST OF ABBREVIATIONS | xi |
| | LIST OF SYMBOLS | xii |
| CHAPTER 1 | INTRODUCTION | 1 |
| | 1.1 Background | 1 |
| | 1.2 Problem Statement | 4 |
| | 1.3 Objective | 6 |
| | 1.4 Scope Of Project | 6 |
| | 1.5 General Methodology | 7 |
| CHAPTER 2 | LITERATURE REVIEW | 9 |
| | 2.1 Reynold Number | 12 |
| | 2.2 Reynold Number and Significant | 11 |
| | 2.3 Critical Reynold Number | 14 |
| | 2.4 Microchannel | 14 |
| | 2.4.1 Application of Microchannel | 15 |

| | | |
|------------------|---------------------------------------|----|
| CHAPTER 3 | METHODOLOGY | 17 |
| 3.1 | Introduction | 17 |
| 3.2 | Flow Chart | 18 |
| 3.2.1 | Pre-processing | 19 |
| 3.2.2 | Solving | 21 |
| 3.2.3 | Post-processing | 23 |
| 3.3 | Developing simulation for CFD | 24 |
| 3.4 | Model or Domain | 24 |
| 3.5 | GAMBIT Meshes | 27 |
| 3.5.1 | Meshing Mode Fluent | 27 |
| 3.6 | Boundary Condition | 28 |
| CHAPTER 4 | RESULT AND ANALYSIS | |
| 4.1 | Introduction | 30 |
| 4.2 | Validation | 30 |
| 4.3 | Mesh Independent test | 33 |
| 4.4 | Temperature Distribution | 36 |
| 4.5 | Flow and heat transfer analysis | 41 |
| 4.5.1 | Boundary layer | 41 |
| 4.6 | Entrance length laminar and turbulent | 45 |
| 4.6.1 | Average Nusselt Number | 46 |
| CHAPTER 5 | CONCLUSION AND RECOMMENDATION | 48 |
| 5.1 | Introduction | 48 |
| 5.2 | Conclusion | 48 |
| | REFERENCE | 50 |

LIST OF FIGURES

| FIGURE | TITLE | PAGE |
|---------------|---|-------------|
| 1.1 | Schematic drawing depicting fluid flow over a flat plate | 2 |
| 1.2 | Prandtl boundary layer concept splits the flow into an outer flow region and a thin boundary layer region | 2 |
| 1.3 | The boundary to compensate for the mass deficit | 3 |
| 1.4 | Flow chart of the general methodology | 7 |
| 3.1 | Flow chart of the methodology | 16 |
| 3.2 | Example of drawing in GAMBIT software | 19 |
| 3.3 | Fluent simulation results for temperature and heat flux | 20 |
| 3.4 | Example of converge iteration | 20 |
| 3.5 | Contour temperature distribution for top and bottom wall | 23 |
| 3.6 | Schematic of rectangular micro-channel heat sink and unit cell. | 24 |
| 3.7 | Isometric view showing the mesh model | 25 |
| 3.8 | Side view of meshed model | 25 |
| 3.9 | Example Drawing using GAMBIT | 26 |
| 3.10 | Example Drawing using GAMBIT with meshing | 26 |
| 4.1 | Comparison of average Nusselts Number | 31 |
| 4.2 | Comparison of Average Temperature Distribution | 31 |

| | | |
|------|--|----|
| 4.3 | Example of setup nodes in meshing the domain | 33 |
| 4.4 | Mesh independent test for Nusselt number laminar and turbulent. | 34 |
| 4.5 | Temperature distribution contour in the x-y plane at channel top wall and bottom wall for laminar flow. | 36 |
| 4.6 | Temperature distribution contour in the x-y plane at channel top wall and bottom wall for turbulent flow | 37 |
| 4.7 | Local temperature distribution contour in the x-z plane (a)middle plane for laminar flow (b) plane sidewall plane for laminar flow | 38 |
| 4.8 | Local temperature distribution in the x-z plane (a) middle plane for turbulent flow (b) sidewall plane for turbulent flow. | 38 |
| 4.9 | Local temperature contours in y-z plane for laminar flow (a) heat sink inlet $x = 0$ mm (b) heat sink middle plane $x = 5$ mm (c) heat sink outlet $x = 10$ mm | 40 |
| 4.10 | Local temperature contours in y-z plane for turbulent flow (a) heat sink inlet $x = 0$ mm (b) heat sink middle plane $x = 5$ mm (c) heat sink outlet $x = 10$ mm | 40 |
| 4.11 | The velocity profile in fully developed for laminar flow | 42 |
| 4.12 | The velocity profile in fully developed for turbulent | 42 |
| 4.13 | Shows the velocity profile in fully developed for laminar and turbulent flow | 43 |
| 4.14 | shows the zooming velocity profile in fully developed for the laminar and turbulent flow | 43 |
| 4.15 | Entry length laminar and turbulent flow Nusselt number | 45 |

LIST OF TABLE

| TABLE | TITLE | PAGE |
|-------|--|------|
| 2.1 | The results of critical Reynolds number in previous researcher. | 15 |
| 3.1 | List of properties | 21 |
| 3.2 | Thermal properties of water | 22 |
| 3.3 | Thermal properties of copper | 22 |
| 3.4 | Dimension of unit cell microchannel | 25 |
| 3.5 | Fluid flow and heat transfer parameters employed in numerical analysis | 29 |
| 3.6 | Continuum type | 29 |
| 3.7 | Boundary Type | 29 |

LIST OF ABBEREVATIONS

| | |
|-----------|--|
| HVAC | Heating Ventilation Air Conditioning |
| GAMBIT | Geometry And Mesh Building Intelligent Tool |
| CFD | Computational Fluid Dynamic |
| CAD | Computer Aided Design |
| CATIA | Computer Aided Three-dimension Interactive Application |
| ANSYS | Analysis System Simulation Software |
| CPU | Central Processing Unit |
| GUI | Graphical User Interface |
| Re | Reynold Number |
| GEO Mesh | Geometric mesh |
| SAT files | Standard ACIS Text |
| ACIS | Andy, Charles, Ian's System |
| CAE | Computer Aided Engineering |
| CAM | Computer Aided Manufacturing |

LIST OF SYMBOL

| | | |
|------------------|---|--------------------------------|
| c | = | Damping coefficient |
| ρ | = | Density |
| μ | = | Viscosity |
| ν | = | Kinematic Viscosity |
| R_{air} | = | Specific gas constant |
| k | = | Specific heat ratio |
| c_p | = | Specific heat |
| c_v | = | Specific heat |
| c | = | Speed of sound |
| v | = | maximum velocity |
| L | = | linear dimension |
| t | = | denotes the time. |
| μ | = | dynamic viscosity of the fluid |
| Re | = | Reynold number |
| d_h | = | hydraulic diameter of channel |

CHAPTER 1

INTRODUCTION

1.1 Background

Boundary layer can define the thickness δ to be the distance across a boundary layer from the wall to a point where the flow velocity has essentially reached the free stream velocity u_0 . Prandtl idea was to divide the flow into two regions. One of that are an outer flow region that is inviscid and irrotational and an inner flow region called a boundary layer a very thin region of flow near a solid wall where viscous forces and rotationally cannot be ignored. The concept of the boundary layer implies that flows at high Reynolds numbers that can be divided up into two unequally large regions. In the bulk of the flow region, the viscosity can be neglected and the flow corresponds to the inviscid limiting solution. This is called the inviscid outer flow. The second region is the very thin boundary layer at the wall where the viscosity must be taken into account. The boundary layer approximation corrects some of the major deficiencies of the Euler equation by providing a way to enforce the no-slip condition at solid walls. Hence, viscous shear forces can exist along walls, bodies immersed in a free stream can experience aerodynamic drag and flow separation in regions of adverse pressure gradient can be predicted more accurately.

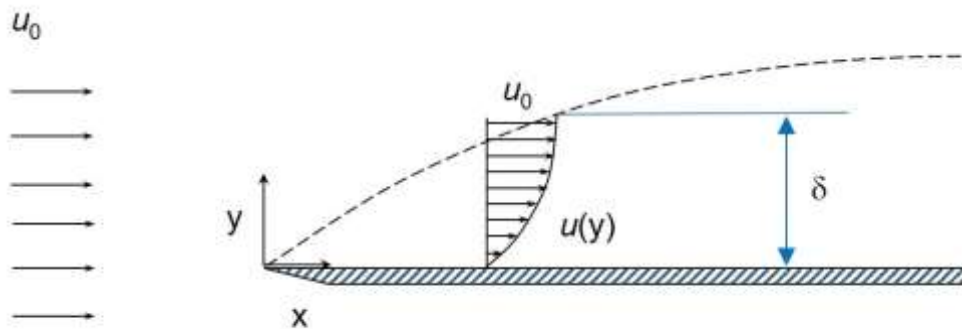


Figure 1.1: Schematic drawing depicting fluid flow over a flat plate.

Has basically achieved the free stream speed converts into a tradition. This thing can happens when the speed has the estimation of 99% of u_0 . Fundamentally, arrange at the divider and look outside it until the point when the speed is that of the unperturbed stream.

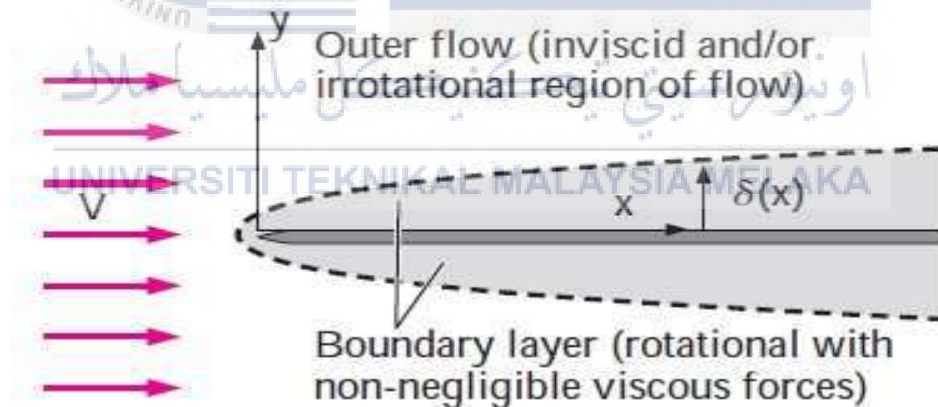


Figure 1.2: Prandtl's boundary layer concept splits the flow into an outer flow region and a thin boundary layer region

The same boundary layer and observe that there is a reduction in the flow rate due to its presence. That reduction is symbolized by the shaded area in the figure. The boundary layer appears due to the shear stress that occurs in the fluid between the layers of the fluid

and between the fluid and the wall. The flow were frictionless inviscid would not lose that mass flow rate. A similar boundary layer and watch that there is a diminished in the stream rate because of its essence. That diminished is symbolized by the shaded region in the figure. The limit layer shows up because of the shear push that happens in the fluid between the layers of the fluid and between the fluid and the divider. If the flow were frictionless inviscid it would not lose that mass flow rate. To obtain in an inviscid flow, an equivalent situation regarding the mass flow rate, move the boundary to compensate for the mass deficit.

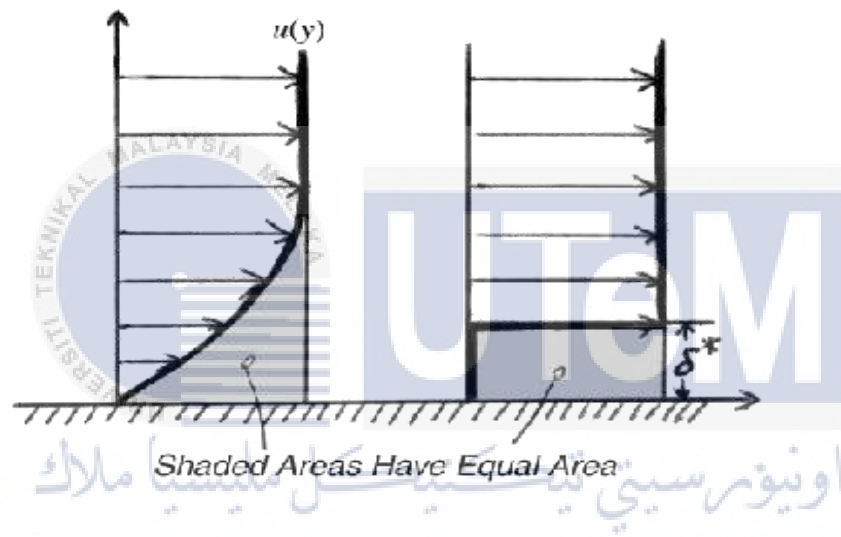


Figure 1.3: The boundary to compensate for the mass deficit

The boundary need to move with a distance such that the mass flow loss from moving the boundary equals the loss in the boundary layer. At the end of the day, the two shaded regions must be equivalent. The distance by which we move the boundary in an inviscid flow to adjust for this no friction assumption is the uprooting thickness. There is something more, it do not lose just mass stream rate when not thinking about the limit layer, but rather it additionally lose force. The separation to represent the loss of energy in the limit layer, when contrasted with that of potential flow. Move the limit by a specific separation can dispose of the limit layer, flow without thickness, and still have a similar force. This separation is the energy thickness.

In this study, the three-dimensional fluid flow and heat transfer in a rectangular microchannel heat sink are analyzed numerically using water as the cooling fluid. The heat sink consists of a 1cm² silicon wafer. The micro-channels have a width of 57 μm and a depth of 180 μm , and are separated by a 43 μm wall. For the micro-channel heat sink investigated, it is found that the temperature rise along the flow direction in the solid and fluid regions can be approximated as linear. For a relatively high Reynolds number of 1400, fully developed flow may not be achieved inside the heat sink. Increasing the thermal conductivity of the solid substrate reduces the temperature at the heated base surface of the heat sink, especially near the channel outlet. (Qu & Mudawar, 2002).

1.2 Problem statement

Critical Reynolds number is important, the critical Reynolds number at which the flow downstream of an orifice or nozzle in a pipe becomes turbulent is an important parameter as it is the demarcating point between purely laminar flow and re-laminar flow.

The value of the critical Reynolds number is estimated for sharp-edged orifices, quadrant-edged orifices and long radius nozzles from indirect evidences using mean flow measurements. The Reynolds number is defined as the ratio of inertial forces to viscous forces and consequently quantifies the relative importance of these two types of forces for given flow conditions. Reynolds numbers frequently arise when performing scaling of fluid dynamics problems and as such can be used to determine dynamic similitude between two different cases of fluid flow. Laminar flow occurs at low Reynolds numbers, where viscous forces are dominant and is characterized by smooth, constant fluid motion. Turbulent flow

Occurs at high Reynolds numbers and is dominated by inertial forces, which tend to produce chaotic eddies, vortices and other flow instabilities. Viscosity is a physical mechanism for smoothing flow variations, there can be a problem differentiating between numerical and physical smoothing. This is especially important when critical Reynolds number situations are encountered, because they require an especially accurate estimate of viscous stresses.

For a laminar boundary layer growing on a flat plate, boundary layer thickness δ is at most a function of V , x , and fluid properties ρ and μ . It is a simple exercise in dimensional analysis to show that δ/x is a function of Re_x . In fact, it turns out that δ is proportional to the square root of Re_x . Infinitesimal disturbances in the flow begin to grow and the boundary layer cannot remain laminar and begins a transition process toward turbulent flow. For a smooth flat plate with a uniform free stream, the transition process begins at a critical Reynolds number, $Re_{x \text{ critical}} \cong 1 \times 10^5$, and continues until the boundary layer is fully turbulent at the transition Reynolds number, $Re_{x \text{ transition}} \cong 3 \times 10^6$. For laminar plate boundary layers the boundary layer thickness can easily be estimated as follows in the boundary layer the inertial forces and the friction forces are in equilibrium. The boundary layer on a plate is laminar close to the leading edge and becomes turbulent further downstream, whereby the position of the transition point x_{crit} can be determined by the critical Reynolds number $Re_{x \text{ crit}}$ given.

1.3 Objective

The objectives of this project are as follows:

1. To determine temperature distribution
2. To find mesh independent test of water flow using laminar and turbulent flow
3. To determine the entrance length
4. To determine the Nusselt number of water flow using laminar and turbulent flow.

1.4 Scope of project

The scopes of this project are:

1. For microchannel, the range critical Reynold number is between 140 to 1000
2. The fluid use is water
3. The hydraulic diameter is 8.658×10^{-5} m for rectangular microchannel
4. The turbulent used is k-epsilon
5. The Reynolds number of water flow is 1000

1.5 General Methodology

The actions that need to be carried out to achieve the objectives in this project are listed below.

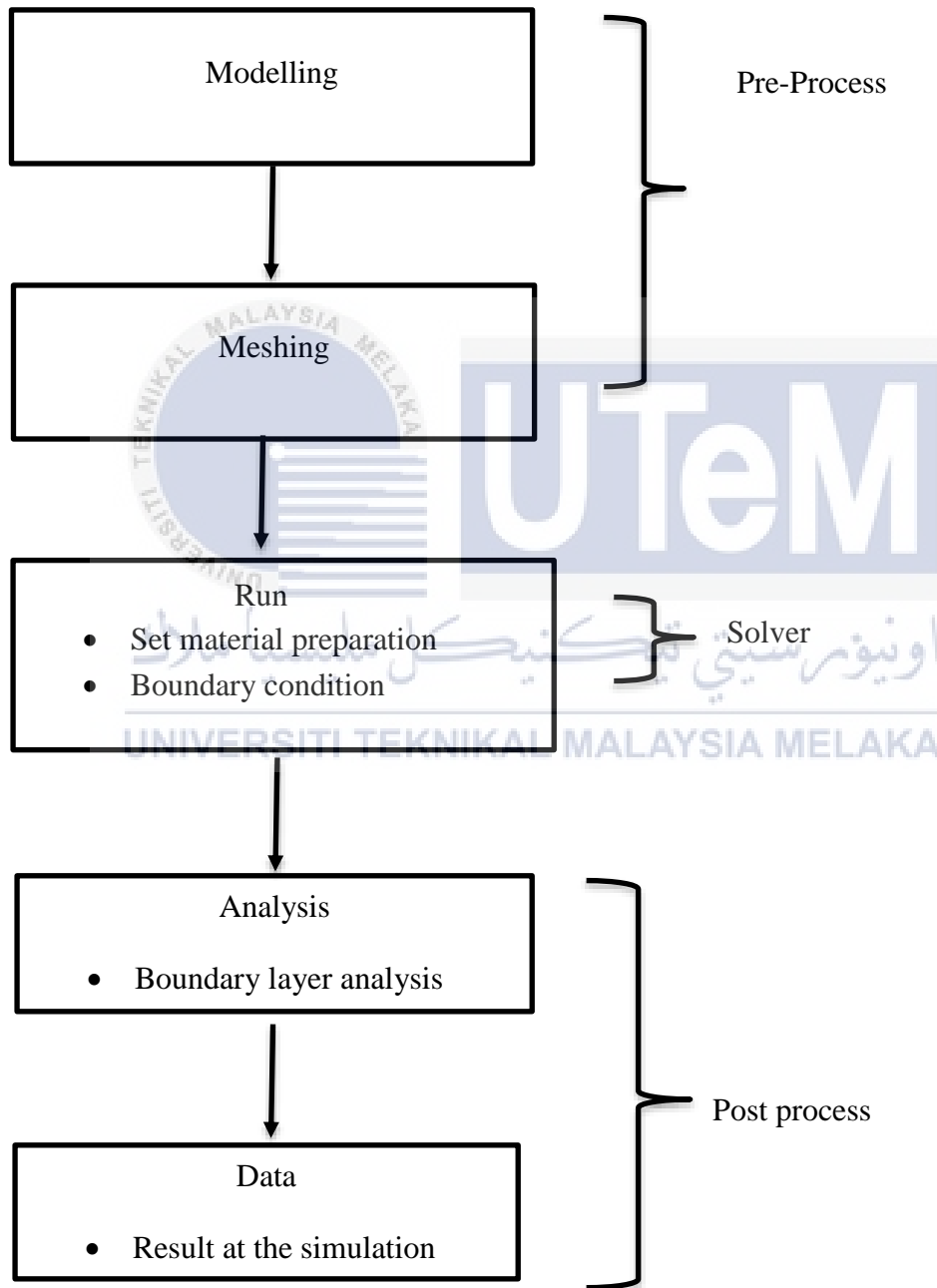


Figure 1.4: Flow chart of the methodology

1. Literature review

Books, journals, article and all other alternative reference for this project will be review.

2. Drawing (pre-processing)

The microchannel

3. Simulation

Simulation of the water velocity profiles using fluent software based on the several of Reynolds number.

4. Report writing

A report on this study will be written at the end of the project.



CHAPTER 2

LITERATURE REVIEW

2.1 Reynolds Number

Critical Reynolds Number in Pipe Flow by Stephen Mirdo (Stephen Mirdo 2010).

The Reynolds number (Re) is an important dimensionless quantity in fluid mechanics used to help predict flow patterns in different fluid flow situations. At low Reynolds numbers flow has a tendency to be commanded by laminar sheet-like flow, however at high Reynolds numbers turbulence comes about because of contrasts in the fluids speed and course, which may once in a while converge or even move counter to the general heading of the stream vortex ebbs and flows.

Hiroaki Nishikawa, Yi Liu (Hiroaki Nishikawa & Yi Liu 2017) hyperbolic advection diffusion schemes for high Reynolds number boundary layer problems. Reynolds number has wide applications, running from fluid flow in a pipe to the entry of air over an air ship wing. It is utilized to predict the progress from laminar to turbulent flow, and utilized as a part of the scaling of comparable however unique measured flow circumstances. The expectations of the beginning of turbulence and the capacity to ascertain scaling impacts can be utilized to help anticipate liquid conduct on a bigger scale, for example, in neighborhood or worldwide air or water development and in this manner the related meteorological and climatological impacts.

Yong-Hui Wang et al. (2017) stated that the Reynolds number is the ratio of inertial forces to viscous forces within a fluid which is subjected to relative internal movement due to different fluid velocities, in which is known as a boundary layer in the case of a bounding surface such as the interior of a pipe. A similar effect is created by the introduction of a stream of higher velocity fluid, such as the hot gases from a flame in air. This relative movement results in fluid friction, which is a factor in building turbulent flow. Balancing this effect is the viscosity of the liquid, which it increases, gradually inhibit turbulence, as more kinetic energy is absorbed by the viscous liquid. The Reynolds number calculates the relative importance of the two types of forces for a particular flow condition and is a guide when turbulent flows will occur under certain conditions.

S. A. Si Salah, E. G. Filali, S. Djellouli (2006). The ability to predict the start of turbulent flow is an important design tool for equipment such as a pipe system or aircraft wing, but the Reynolds number is also used in fluid dynamics scale scales, and is used to determine the dynamic equations between two types of fluid flow cases, such as between aircraft models, and its full size version. Such grading is not linear and the use of the Reynolds number for both conditions allows the scale factor to be developed. Laminar flow occurs at low Reynolds numbers, where the viscosity is dominant, and is characterized by continuous constant fluid motion. Turbulent flows occur at high Reynolds numbers and are dominated by inertial forces, which tend to produce stirring eddies, vortices and other flow instability. The Reynolds number is defined as

$$Re = \frac{\rho v \mathcal{L}}{\mu} = \frac{v \mathcal{L}}{\nu}$$

ρ is the density of the fluid . SI units is kg/m^3

v is the velocity of the fluid with respect to the object. SI units is m/s

L is a characteristic linear dimension. SI units is m

μ is the dynamic viscosity of the fluid. SI units is Pa·s or N·s/m² or kg/m·s

ν is the kinematic viscosity of the fluid . SI units is m²/s.

The Reynolds number can be characterized for a few unique circumstances where a fluid is in relative motion to a surface. These definitions by and large incorporate the fluid properties of density and viscosity, plus a velocity and a characteristic length or characteristic dimension \mathcal{L} . For aircraft or ships, length or width may be used. For flow in pipes or spheres moving in liquids, inner diameter is usually used today. Other shapes such as rectangular plates or non-spherical objects have the same diameter. For custom density liquids such as viscosity gas or liquid fluid such as non-Newtonian fluids, special regulations apply. Velocity can also be a problem in some situations, especially the stirred vessels. The form of the Reynolds number can be derived as follows

$$Re = \frac{\text{inertial forces}}{\text{viscous forces}} = \frac{\text{mass} \times \text{acceleration}}{\text{dynamic viscosity} \times \frac{\text{velocity}}{\text{distance}} \times \text{area}}$$

$$Re = \frac{\rho \mathcal{L}^3 \frac{v}{t}}{\mu \left(\frac{v}{\mathcal{L}}\right) \mathcal{L}^2} = \frac{\rho \mathcal{L}^3 \frac{1}{t}}{\mu \left(\frac{1}{\mathcal{L}}\right) \mathcal{L}^2} = \frac{\rho \mathcal{L}^2 \frac{1}{t}}{\mu} = \frac{\rho \frac{\mathcal{L}}{t} \mathcal{L}}{\mu} = \frac{\rho v \mathcal{L}}{\mu} = \frac{v \mathcal{L}}{\nu}$$

Where:

v is the maximum velocity of the object relative to the fluid. SI units is m/s.

\mathcal{L} is a characteristic linear dimension, (travelled length of the fluid; hydraulic diameter when dealing with river systems) (m)

t denotes the time.

μ is the dynamic viscosity of the fluid. SI unit is Pa·s or N·s/m² or kg/m·s

ν (nu) is the kinematic viscosity ($\nu = \mu/\rho$) SI unit is m²/s.

ρ is the density of the fluid. SI unit is kg/m³.

2.2 Reynold number and Significant

There are many experimental research that have been done by researchers in configuring fluid flow and thermal conductivity inside microchannel. Experiments on transport in micro-channel a critical review have been done by S. V. Garimella and C. B. Sobhan in 2003. Investigations focused on understanding the fundamentals of microchannel flow, and on comparing and contrasting the flow and heat transfer characteristics in microchannel with those in conventional channels. The two important objectives in electronics cooling, namely the reduction of the device maximum temperature and the minimization of temperature gradients on the device surface, can be efficiently achieved by the use of microchannel heat sinks. Reynolds number of approximately 400.

(Peiyi and Little, 1983) has detailed that there are many factors in which influencing the fluid flow and in the meantime influencing the estimation of the grating element in microchannel. Surface roughness is one of the elements that influences the fluid flow from transition to turbulent for the most part by expanding of drag coefficients in turbulent flow in microscale channel. For this situation, critical roughness is displayed yet rubbing factors measured in smooth channel concurred with macroscale hypothesis in rectangular microchannel. Along these lines, influencing the grating to factor too little that it can be reliable in this microchannel. Additionally, contact factor is relied upon Reynolds number.

Analysis of three-dimensional heat transfer in micro-channel heat sink by Weilin Qu, Issam Mudawar (Qu & Mudawar, 2002) are analyzed numerically using water as the cooling fluid. The code is carefully validated by comparing the predictions with analytical solutions and available experimental data. The single-phase forced convective heat transfer of water in rectangular channels with hydraulic diameter ranging from 133 to 367 μm . Increasing Reynolds number increases the length of the developing region. Fully developed flow may not be achieved inside the heat sink for high Reynolds numbers. This results in enhanced heat transfer, alas at the expense of a higher pressure drop.

Experiments on flow characteristic at very low Reynolds numbers for liquid flow in microchannel have been done by Xiwen Zhang (X. Zhang et al., 2016). They tested deionized water and kerosene in rectangle cross-section microchannel with width 2.7 – 20 μm and depth of 20 – 45 μm under very low Reynolds number condition ($10^{-5} < \text{Re} < 10^{-2}$) thus provide a correlation to the flow of Newtonian fluid in a smooth micrometer-sized consistent with classical theory of laminar flow.

(Kim, 2016) Byongjoo Kim has played out an investigation to investigate the legitimacy of hypothetical relationships in anticipating fluid flow and heat transfer attributes in light of customary measured of microchannel. 10 different rectangular microchannels with water driven breadth of 155 – 580 μm and Reynolds number going from 30 to 2500 are tried or tested. The basic Reynolds number of 1700 to 2400 are gotten with decrease of viewpoint proportion from 1.0 to 0.25. The single stage laminar grinding factors in the microchannel has obeyed to the ordinary Poiseuille flow theory.

2.3 Critical Reynolds number

Critical Reynolds number is defined as the Reynolds number, above which the flow becomes turbulent. Below a lower critical value of Reynolds number flow is laminar or streamline, above a higher critical value flow is turbulent or sinuous in Reynolds terminology. Between these values the flow is in what is called transition. The higher critical value is strongly dependent on upstream conditions. Reynolds observed values of between 11,800 and 14,300 for water in bell mouth tubes of a few centimeters diameter. The lower critical value is less sensitive and is usually quoted simply as the critical Reynolds number. Its value for smooth circular pipes and tubes is approximately 2,000.

2.4 Microchannel

The combination between these two microchannel and Nano fluid contribute high coefficient heat transfer (A.A. Hussien et al.2016). Microchannel is another new technology with the smallest size which can remove a large amount of heat from a small region (Qu & Mudawwar, 2002). This microchannel also can help engineer or technicians to use only small space for electronic device especially during installation. Microchannel has the smallest size and light as compared to macrochannel and high in demands of low inventory of coolant and high coefficient of convection heat transfer (Y.F. Li al, 2016).

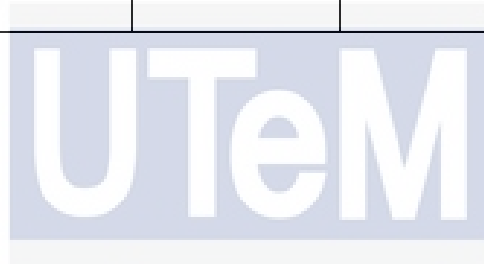
2.4.1 Application of Microchannel

Microchannel works as passaging flow for cooling liquid since it combines the attributes of high surface area to volume ratio, small mass and volume and small coolant merchandise (Qu & Mudawwar, 2002). Microchannel as cooling technology involve the process of removing heat from a small region is suitable for a computer which consist processor from the motherboard cpu which produce high heat.

Table 2.1: The result of critical Reynolds determined by previous researchers.

| Author | Testing fluid | Hydraulic Diameter | Geometry | Remarks |
|-----------------------|---------------|----------------------|-------------|--|
| (Qu & Mudawwar, 2002) | water | 86.58 μm | rectangular | Much higher average heat flux and Nusselt number can be found in the region near the channel inlet and decrease rapidly to nearly constant values. |
| (Zhu, 2006) | water | 153 μm | Rectangular | The average heat flux at the channel top wall is slightly larger than at the bottom wall, but the corresponding average Nusselt numbers are virtually identical. |
| (Yuan et al, 2016) | Water | 10mm diameter length | Circular | Reynold number range for transition flow become narrower with decreasing tube diameter. |

| | | | | |
|----------------------|-------|-------------|-------------|---|
| (Dirker et al, 2014) | Water | 0.57 mm | Rectangular | For most of the channel length, the average heat flux and Nusselt number at the channel top and bottom walls are about half their corresponding values at the channel side wall |
| (Pfund et al, 200) | Water | 252 μ m | Rectangular | Transition value was lower than conventional critical Reynolds number |



اونيورسيتي تيكنيكل مليسيا ملاك

UNIVERSITI TEKNIKAL MALAYSIA MELAKA

CHAPTER 3

METHODOLOGY

3.1 Introduction

This study is conducted by doing some validation in previous journal of Qu and Mudawar (2002) in order to accomplish this project objectives. A simulation of water flow through a single micro-size channel is done. GAMBIT is geometry and mesh generation software for computational fluid dynamics (CFD) analysis. GAMBIT has a single interface for geometry creation and meshing that brings together several pre-processing technologies in one environment. Advanced tools for journaling let edit and conveniently replay model building sessions for parametric studies. GAMBIT can import geometry from virtually any CAD/CAE software in Para-solid, ACIS, STEP, IGES, or native CATIA V4/V5 formats. After drawing and meshing domain in the GAMBIT software, the simulation have been conduct to get the result using Fluent 6.1 software.

3.2 Flow chart

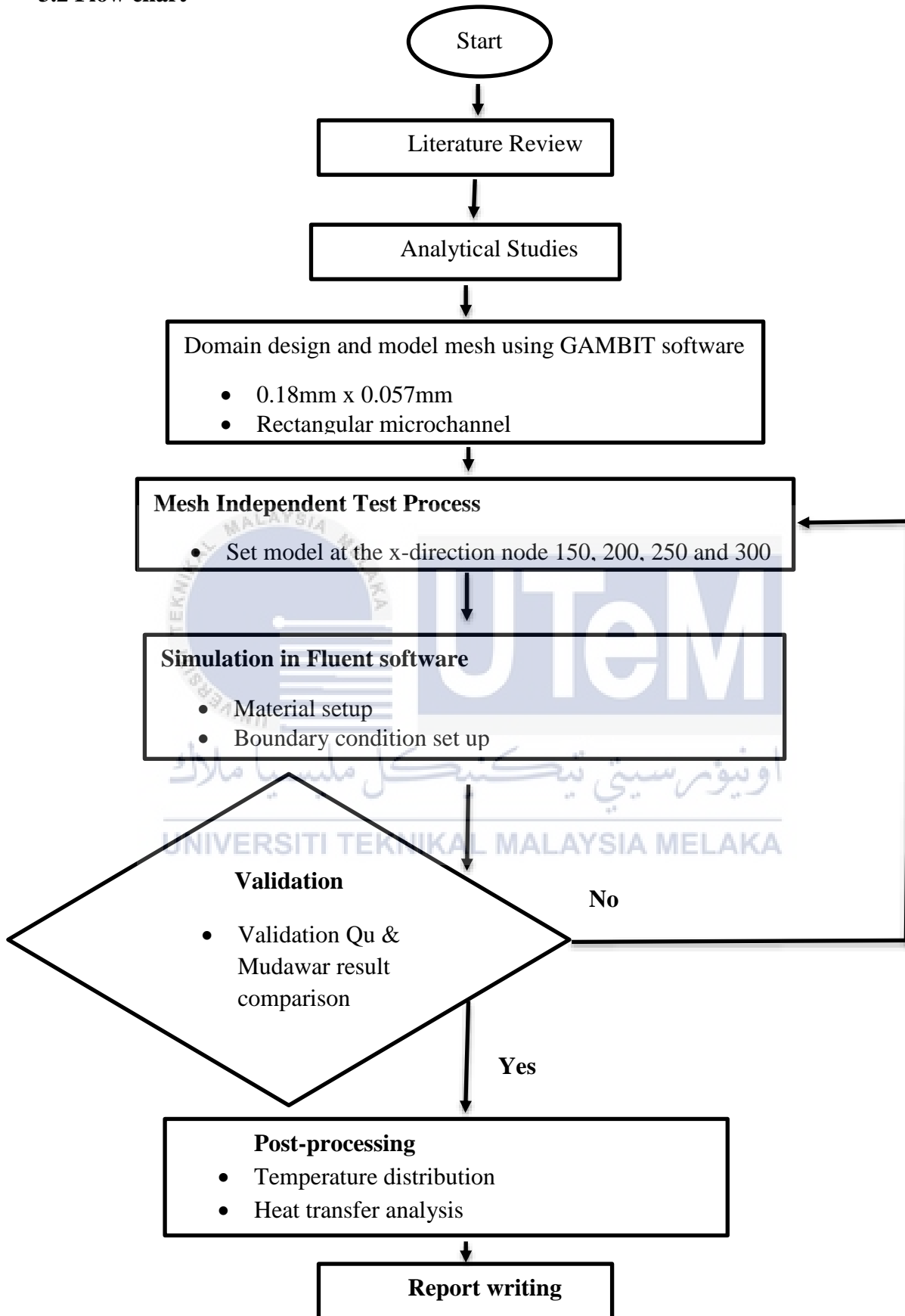


Figure 3.1: Shows the flow chart

3.2.1 Pre-processing

There are three stages in a computational fluid dynamic (CFD) simulation to achieve this project objective which are pre-processing, solving and lastly post-processing. Pre-processing is a formulation of the problem which consist of governing equation and the boundary condition. It is also a construction of computational mesh which is set of control volumes. Pre-processing steps is started with the geometry by sketching the rectangular micro-channel heat sink with dimension of 0.9mm x 0.1mm x 10 mm at the outside and 0.18mm x 0.057mm x 10mm rectangular micro-channel as for the inside. The projection line is sketched in order to project 3D rectangular onto a plane with 8 edges on faces and one target body which outside the rectangular.

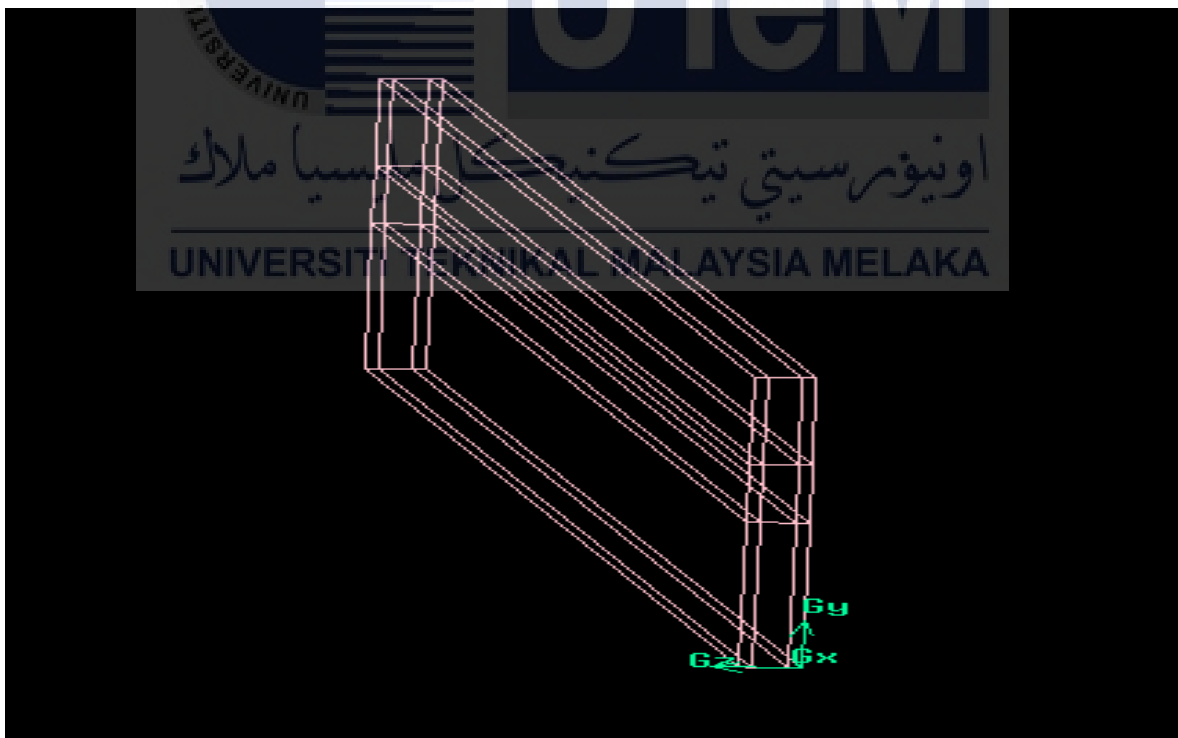


Figure 3.2: Example of drawing in GAMBIT software

The simulation have been conducted after finish use GAMBIT software to drawing and apply meshing to the domain. The simulation processing have been apply the material setup for water and copper. The boundary condition setup also need to apply for choosing the inlet, outlet, wall and all the views. After done with the setup, iteration must be apply to run the simulation. 1000 iteration have been apply to all the simulation that have been conduct. Figure 3.3 and Figure 3.4 show the example of fluent simulation results.



Figure 3.3: Example of fluent simulation result for temperature and heat flux

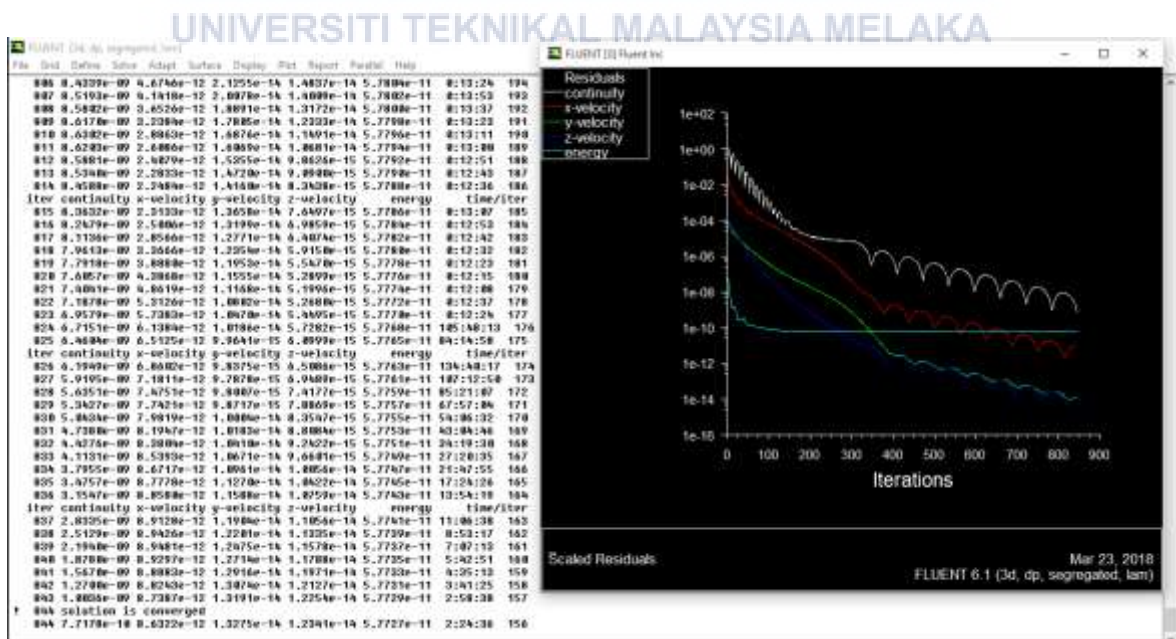


Figure 3.4: Example of converge iteration

3.2.2 Solving

Solving by discretization of the governing equations and solution of the resulting algebraic equations.

Table 3.1: List of properties

| Symbols | Properties | Formula |
|--------------------|--------------------------|---|
| ρ | Density | Kg/m^3 |
| μ | Viscosity | Kg/m.s |
| ν | Kinematic Viscosity | m^2/s |
| R_{air} | Specific gas constant | kJ/kg.K $\text{m}^2\text{s}^2.\text{K}$ |
| k | Specific heat ratio | c_p/c_v |
| c_p | Specific heat | kJ/kg.K $\text{m}^2\text{s}^2.\text{K}$ |
| c_v | Specific heat | kJ/kg.K $\text{m}^2\text{s}^2.\text{K}$ |
| c | Speed of sound | m/s |
| $\frac{\delta}{x}$ | Boundary Layer Thickness | Laminar = $\frac{4.91}{\sqrt{Re_x}}$ Turbulent = $\frac{0.16}{(Re_x)^{1/7}}$ |

Table 3.2: Thermal properties of water

| | |
|--|----------|
| Density (kg/m ³) | 998.2 |
| C _p (specific heat)(j/kg.k) | 4182 |
| k, Thermal Conductivity (w/m.k) | 0.6 |
| μ, Viscosity (kg/m.s) | 0.001003 |

Table 3.3: Thermal properties of copper

| | |
|--|-------|
| Density (kg/m ³) | 8978 |
| C _p (specific heat)(j/kg.k) | 381 |
| k, Thermal Conductivity (w/m.k) | 387.6 |

3.2.3 Post-Processing

Post-processing which is an analysis of results that consist of calculation of derived quantities such as force, flow rate and else. It also produces visualization like graph and plots of the solution. The mesh independent test have been conducted. The data and result have been concluded. To reduce time and iteration of the convergence as low as can and to get the best meshing with the lowest nodes, a mesh independent test is stimulating. The temperature distribution at several x–y planes, namely the heat sink top wall, channel top wall, channel bottom wall, and heat sink bottom wall is illustrated.



Figure 3.5: Example of contour temperature distribution for top and bottom wall

3.3 Developing Simulation for CFD

The process in developing simulation for CFD was started by using fluid flow Fluent which consist of geometry, meshing setup, solution and result in GAMBIT since it is one project management tools that can handles the passing data between those tools. All basic work flow was explained in this project.

3.4 Model or Domain

Model pre-processing drawing was follow Qu & Mudawar (2002) journal title analysis of three-dimensional heat transfer in micro-channel heat sink , step is started with geometry by sketching the rectangular microchannel heat sink with dimension have a width of $57 \mu\text{m}$ and a depth of $180 \mu\text{m}$, and are separated by a $43 \mu\text{m}$ wall. The channels had a width of $50 \mu\text{m}$ and a depth of $302 \mu\text{m}$, and were separated by $50 \mu\text{m}$ thick walls. The micro-tube had an inner diameter of $902 \mu\text{m}$, wall thickness of $89 \mu\text{m}$ and length of 5.8 mm .

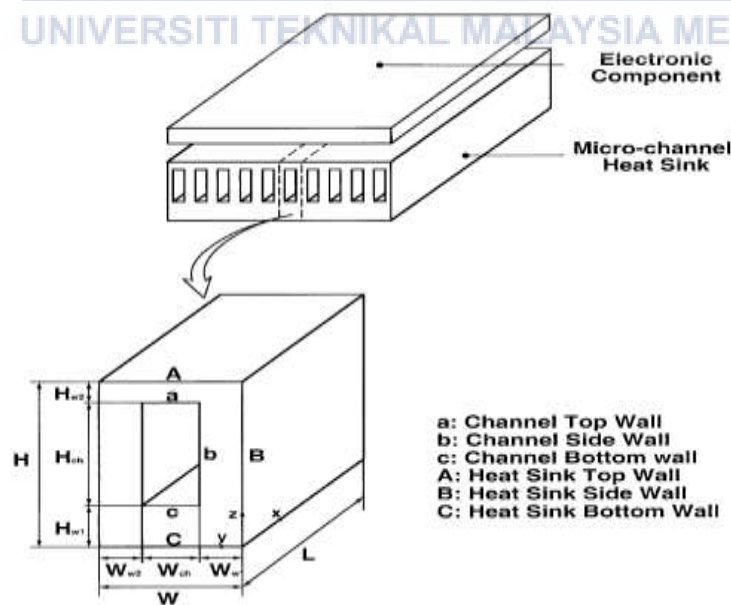


Figure 3.6: Schematic of rectangular micro-channel heat sink and unit cell.

Table 3.4 : Dimension of unit cell of microchannel

Dimensions of unit cell of micro-channel heat sink

| W_{w1} (μm) | W_{ch} (μm) | W_{w2} (μm) | H_{w1} (μm) | H_{ch} (μm) | H_{w2} (μm) | L (mm) |
|-------------------------------|-------------------------------|-------------------------------|-------------------------------|-------------------------------|-------------------------------|-------------|
| 21.5 | 57 | 21.5 | 270 | 180 | 450 | 10 |

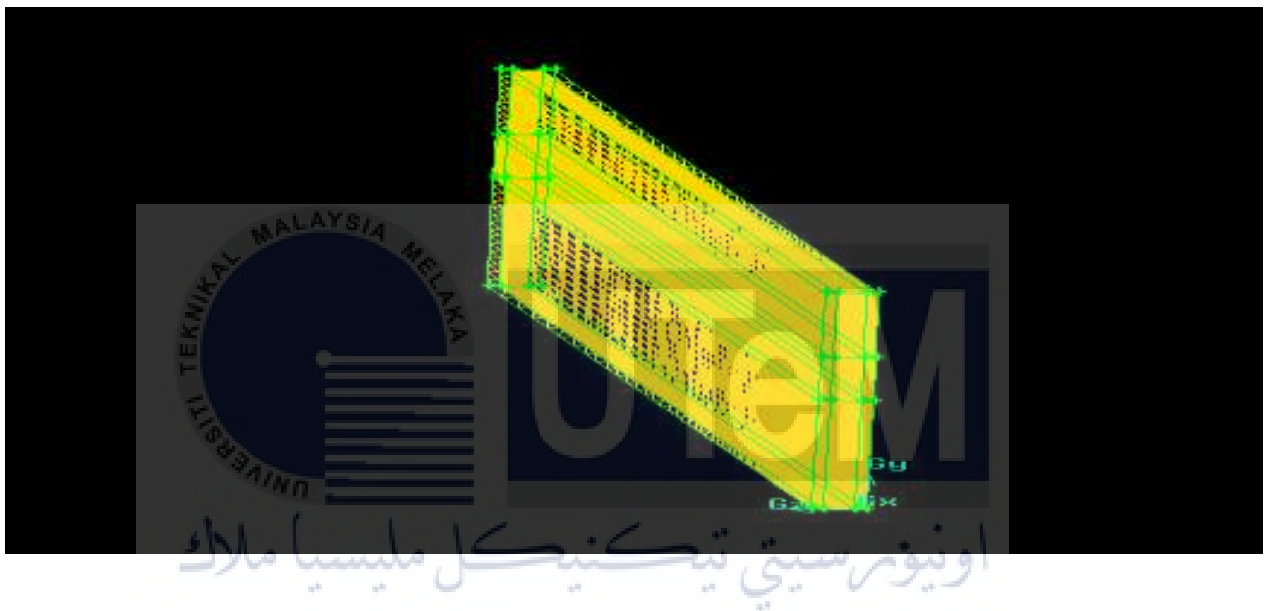


Figure 3.7: Isometric view showing the mesh model

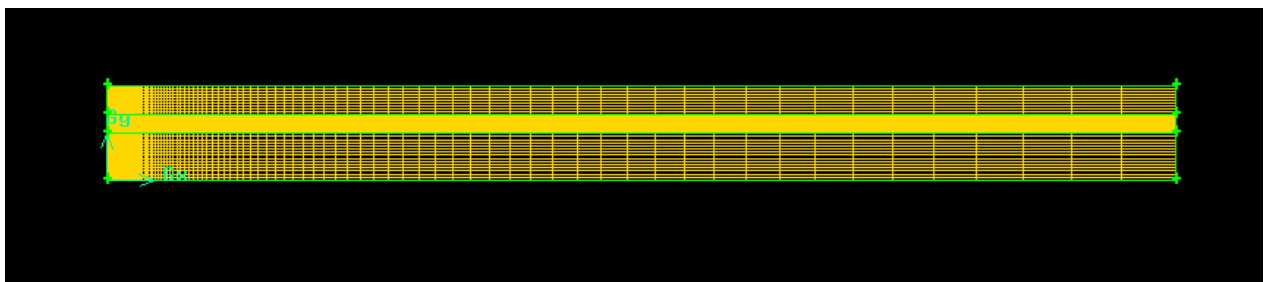


Figure 3.8: Side view of meshed model

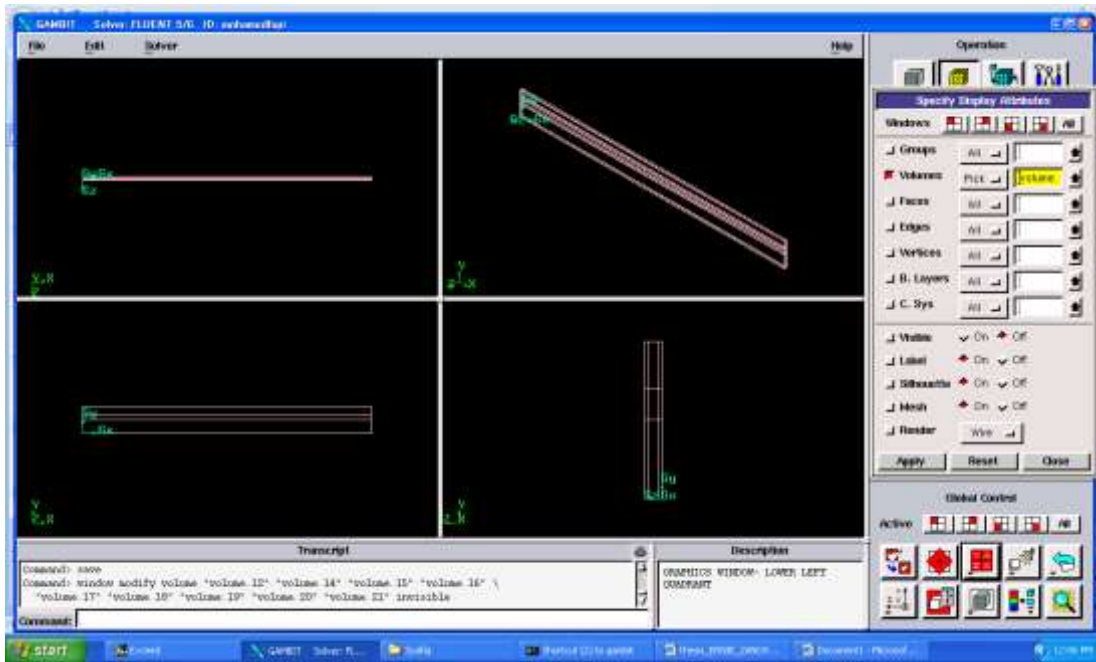


Figure 3.9: Example Drawing using GAMBIT

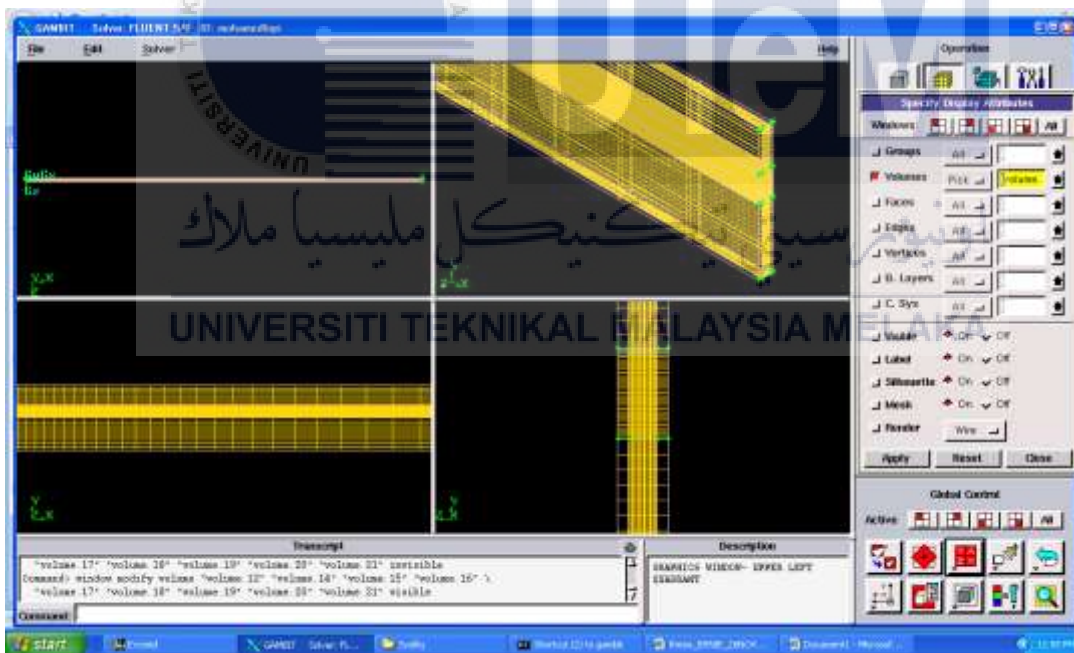


Figure 3.10: Example Drawing using GAMBIT with meshing

3.5 GAMBIT Meshes

GAMBIT can create both surface and volume meshes. Meshes from Third-Party CAD Packages. Import grid files from third party CAD packages by using the items in the File Import menu. Alternatively, the feral filter enables you to convert files created by several finite element packages to the grid file format used by Fluent.

3.5.1 Meshing mode Fluent

Functions as a robust, unstructured volume mesh generator. Generates volume meshes that can be transferred to solution mode in Fluent. Uses the Delaunay triangulation method for tetrahedral. The advancing layer method use for prisms and generates hex core mesh. Has a robust surface wrapper tool includes size functions that can produce ideal size distributions for many CFD calculations and can directly create a hex dominant mesh on faceted geometry using the cut cell mesh. Has tools for checking, repairing, and improving boundary mesh to ensure a good starting point for the volume mesh and can manipulate face cell zones. Is flexible it allows the most appropriate cell type to be used to generate the volume mesh. Tet meshes are suitable for complex geometries.

3.6 Boundary Condition

Qu & Mudawar,(2002) analysis of three-dimensional heat transfer in micro-channel heat sinks for boundary can be specified as follows, the hydraulic boundary conditions, the velocity is zero at all boundaries except the channel inlet and outlet. A uniform velocity is applied at the channel inlet.

$$u = \frac{Re \cdot \mu_f}{d_h}, v = 0, w = 0,$$

The flow is fully developed at the channel outlet.

$$\frac{\partial u}{\partial x} = 0, \frac{\partial v}{\partial x} = 0, \frac{\partial w}{\partial x} = 0,$$

For the thermal boundary conditions, adiabatic boundary conditions are applied to all the boundaries of the solid region except the heat sink top wall, where a constant heat flux is assumed.

$$-k_s \frac{\partial T}{\partial z} = q'',$$

At the channel inlet, the liquid temperature is equal to a given constant inlet temperature.

$$T = T_{in}$$

The flow is assumed thermally fully developed at the channel outlet.

$$\frac{\partial^2 T}{\partial x^2} = 0,$$

It should be noted here that the temperature field may not be fully developed if the entrance length is longer than the channel length, as demonstrated later in this paper. However, the change of temperature gradient along the flow direction at the channel exit is usually very small even for very large Reynolds numbers.

Table 3.5: Fluid flow and heat transfer parameters employed in numerical analysis

| Re | T_{in} (°C) | q'' (W/cm ²) | k_{water} (W/m °C) | $k_{silicon}$ (W/m °C) | k_{copper} (W/m °C) |
|-------|------------------|-------------------------------|-------------------------|---------------------------|--------------------------|
| 140.0 | 20.0 | 90.0 | 0.61 | 148.0 | 401.0 |

Table 3.6: Continuum type

| Name | Type |
|--------|-------|
| Water | Fluid |
| Copper | Solid |

Table 3.7: Boundary Type

| Name | Type |
|------------|------|
| Inlet | Wall |
| Outlet | Wall |
| Topwall | Wall |
| Bottomwall | Wall |

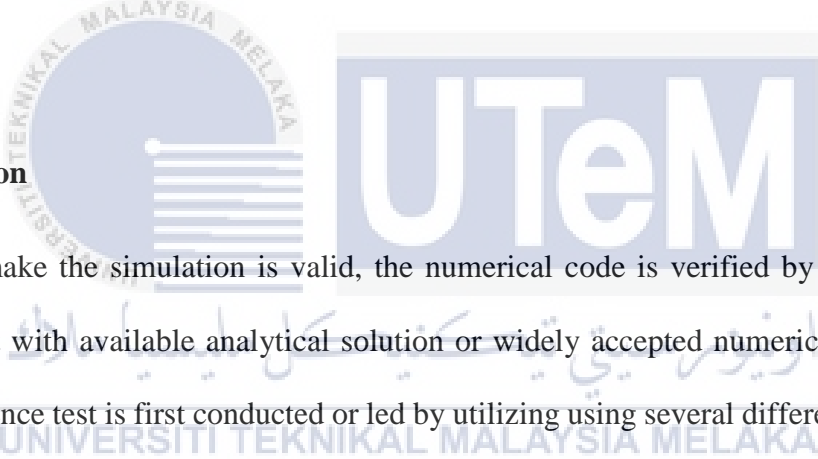
CHAPTER 4

RESULTS AND ANALYSIS

4.1 Introduction

In this section, the validation of the simulation is done and the consequence of the simulation will be appeared and discussed. The Nusselt number along the channel is recognized to plot a graph chart and demonstrate the impact of the outline cooling impact.

4.2 Validation



To make the simulation is valid, the numerical code is verified by contrasting or comparing it with available analytical solution or widely accepted numerical results. The grid dependence test is first conducted or led by utilizing using several different mesh sizes. This test proved that the results based on the final grid system presented in this paper are independent of mesh size. The solution for the energy equation was also verified. The surrounding solid region is evacuated and a pure convective heat transfer problem in the rectangular channel is considered. The boundary condition is chosen as constant longitudinal wall heat flux with uniform peripheral heat flux. The Reynolds number is set to 140 for validation. Based on the numerical results, the average peripheral Nusselt number Nu is evaluated and plotted in figure against the length of the microchannel, L .

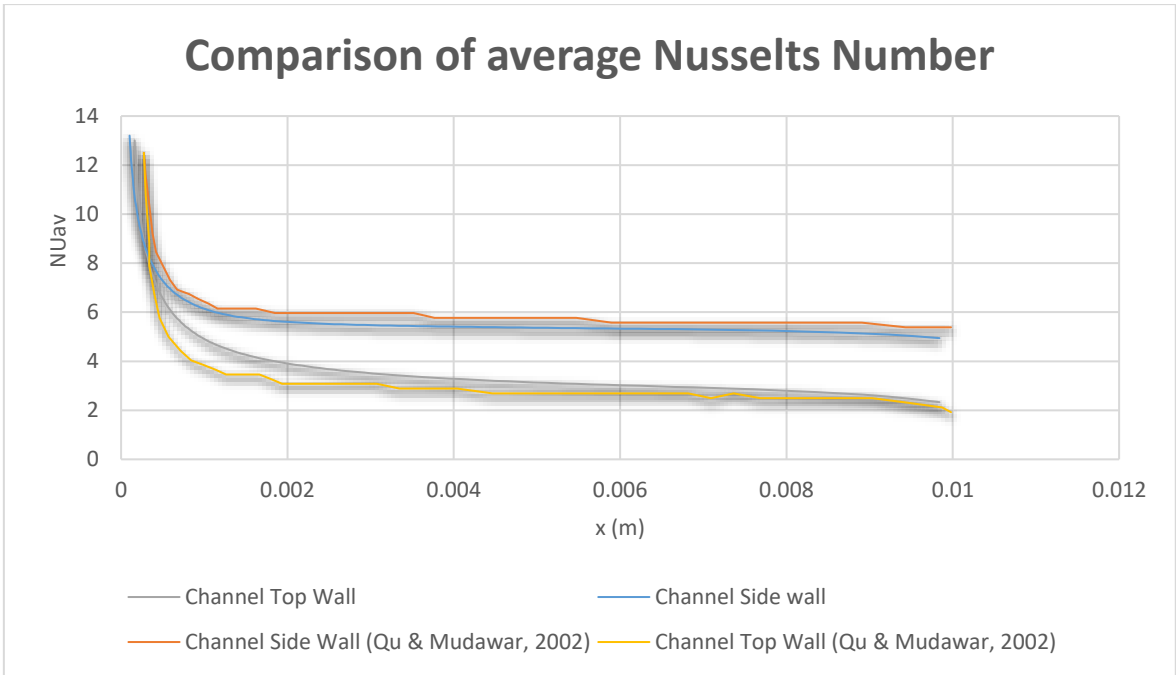


Figure 4.1: Comparison of average Nusselts Number

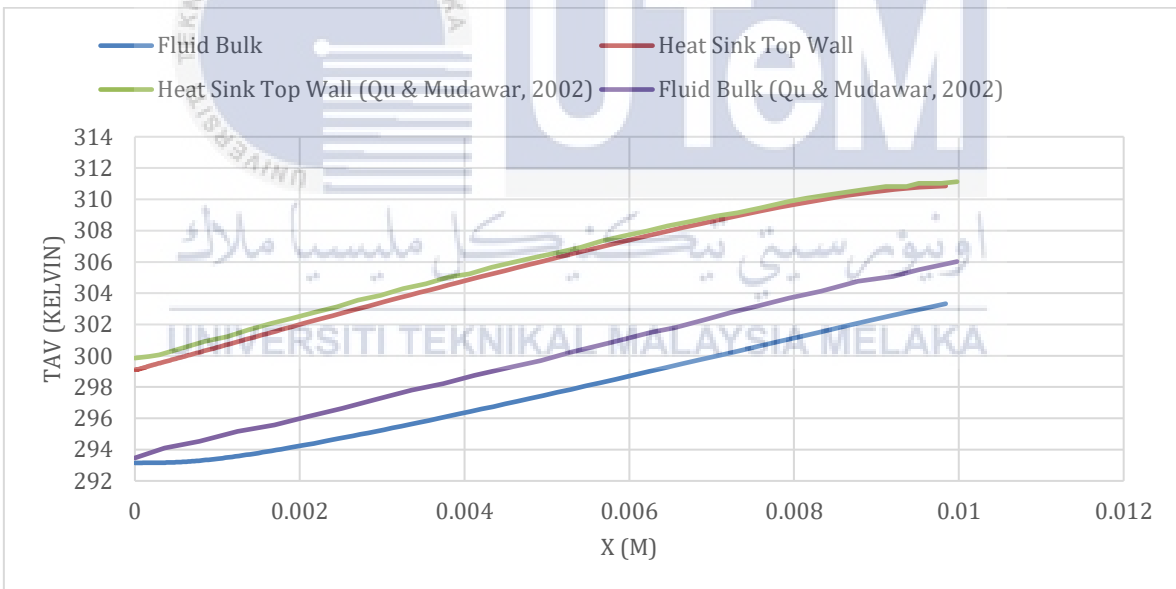


Figure 4.2: Comparison of Average Temperature Distribution

Nu is calculated using formula below

$$Nu = \frac{q'' Dh}{k(T_s - T_m)}$$

Where $T_{\Gamma,m}$ is the average temperature at the line side wall of the boundary,

$$T_{\Gamma,m} = \frac{1}{\Gamma} \int T_{\Gamma} \delta\Gamma$$

and T_m is the fluid bulk temperature,

$$T_m = \frac{\int_{A_c} ut \, dA_c}{\int_{A_c} u \, dA_c}$$

The outcomes shows that, the simulation result for the present straight microchannel heat sink is consequence or similar to the result of Qu and Mudawar, where Nusselt number is high at the inlet, but drop rapidly and approaches constant value at fully develop value. The result from the calculation is utilized to compare with the work of Qu and Mudawar which is also plotted in Figure 4.1 and Figure 4.2. The largest deviation between simulation result from Qu and Mudawar result is 13.1%. In this manner, the simulation is considered as valid since the simulation is showing the identical pattern as Qu and Mudawar works. This proves that the simulation for other design are acceptable as well. The deviation of Nusselt number between simulations and Qu & Mudawar at the fully developed region is about 8.16%.

4.3 Mesh Independent Test

The design that has been doing for this project is based on Qu and Mudawar journal which is the node have been change to test the boundary layer. It is important that the solution is the numerical solution to the problem that posed by defining the mesh and boundary conditions. The more accurate the mesh and boundary conditions, the more accurate converged solution will be. Convergence that the way generally define convergence by looking at Residual values is only a small part of ensuring that have a valid solution. For a steady state simulation needs to ensure that the solution satisfies the following three conditions which is the Residual RMS Error values have reduced to an acceptable value with typically 10^{-4} or 10^{-5} . Mesh Independent Test below show node of meshing in GAMBIT



Figure 4.3: Example of setup nodes in meshing the domain

This simulations study was performed with four different meshes size at the channel side wall which is y-direction of the fluid wall. The different meshes sizes are $40 \times 25 \times 150$, $45 \times 25 \times 150$, $50 \times 25 \times 150$ and $55 \times 25 \times 150$. Figure 4.3 shows the meshing independences test for isometric and front for the channel side wall.

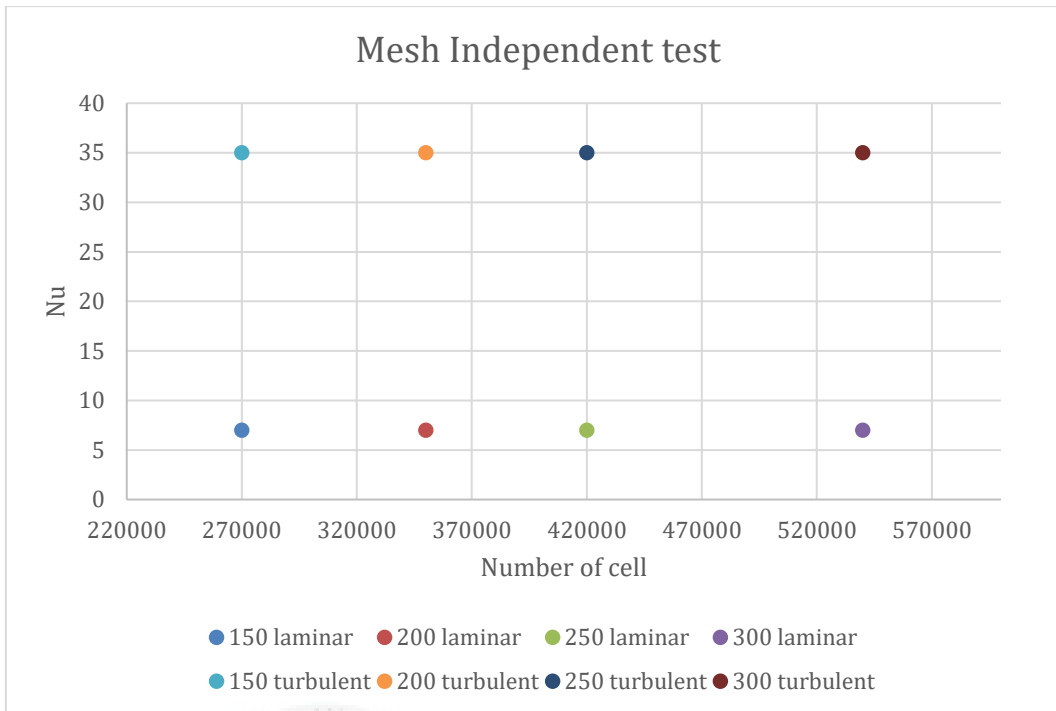


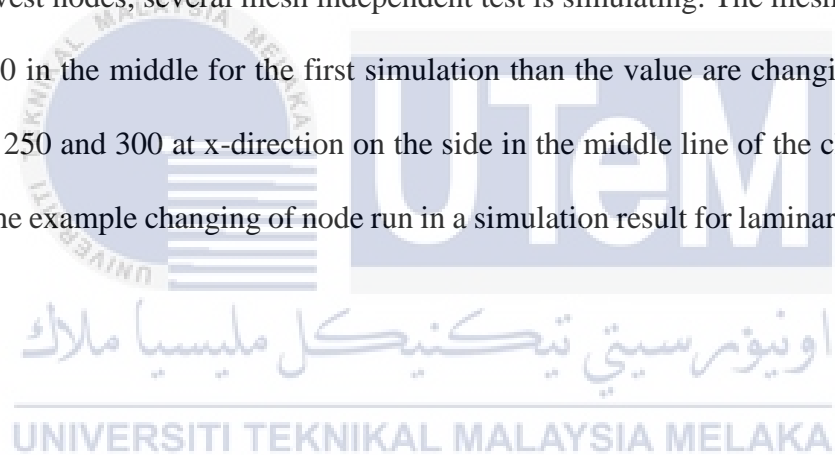
Figure 4.4: Mesh independent test for Nusselt number laminar and turbulent

The values of interest are essentially the main outputs from the simulation, so pressure drop, forces, mass flow and others. Need to be make sure that these have converged to a steady value otherwise if let the simulation run for an additional 50 iterations then the simulation would have a different result. Mesh independent test are analyzed to establish the accuracy of the simulation. The simulation are with same Reynolds number which 1000 and velocity 11.606 after calculate with formula.

Ensuring that these values have reached a steady solution means that basing decisions on a single repeatable value. Generally speaking, need to be ensure that before beginning a simulation need to clearly define what the values of interest are and need to make sure that the simulation have to monitor these to ensure that the simulation reach a steady state. The best way to check for a mesh independent solution is to plot a graph of the resultant monitor value against the number of cells in your simulation. This is illustrated below where the three

results from the steady monitor points for the average temperature at an outlet. By increasing the mesh size further the simulation that the 8 million cell simulation results in a value that is within acceptable range. This indicates that the simulation have reached a solution value that is independent of the mesh resolution, and for further analysis simulation can use the 6 million cell case, as it will give us a result within the user defined tolerance. The grid dependence test is first directed by utilizing a few different mesh sizes. This test demonstrated that the outcomes based on the final grid system presented in this paper are independent of mesh size.

To get best time and iteration of the convergence as low as can and great meshing with the lowest nodes, several mesh independent test is simulating. The meshing nodes was set up at 150 in the middle for the first simulation than the value are changing from value 150 to 200, 250 and 300 at x-direction on the side in the middle line of the channel. Figure 4.4 shows the example changing of node run in a simulation result for laminar and turbulent.



4.4 Temperature Distribution

The temperature distribution contour at several x–y planes, namely the heat sink top wall, channel top wall, channel bottom wall, and heat sink bottom wall is illustrated in Figure 4.5 and Figure 4.6. Some interesting features are readily observed. From the distribution of constant temperature contour lines, the temperature gradient decreases along the longitudinal x-direction from the channel inlet to the outlet. However, the change of gradient is so small that a linear temperature rise is a good approximation for the situation studied. From the distribution temperature of constant temperature contour lines, along with the longitudinal x-direction, the temperature gradient decrease from the channel inlet to outlet for both channel top and a bottom wall.

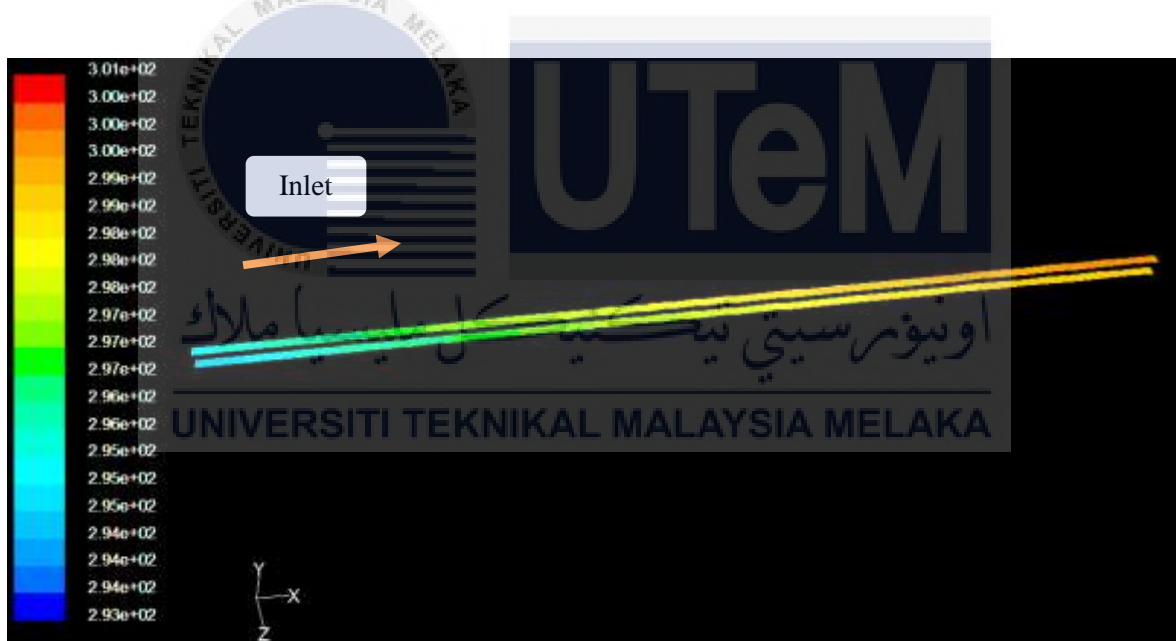


Figure 4.5: Temperature distribution contour in the x-y plane at channel top wall and bottom wall for laminar flow

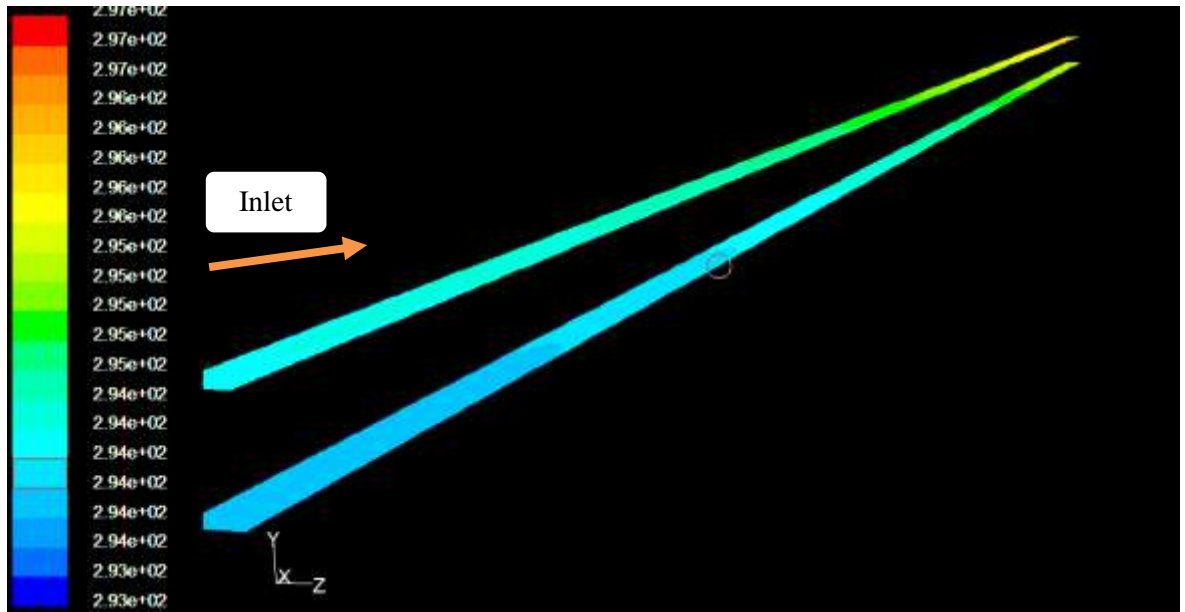


Figure 4.6: Temperature distribution contour in the x-y plane at channel top wall and bottom wall for turbulent flow

The temperature along the transverse y-direction is virtually constant. The temperature decreases from the heat sink top wall to the heat sink bottom wall. The shape of the channel is clearly visible due to the large difference in temperature gradient between the solid and liquid. Because of the copper high thermal conductivity, the temperature gradient in the copper is much smaller than that in water. The top wall line temperature and sidewall line temperatures, middle line temperature and bottom wall are plotted in Figure 4.7 until Figure 4.10.

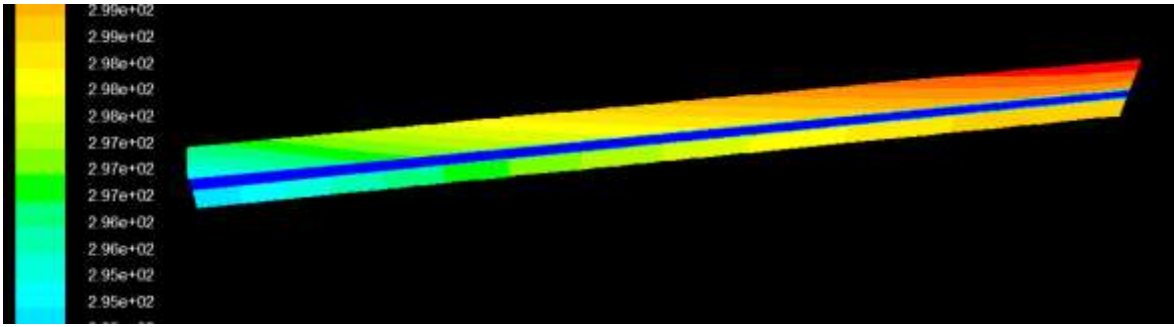


Figure 4.7: Local temperature distribution contour in the x-z plane
 (a) Middle plane for laminar flow

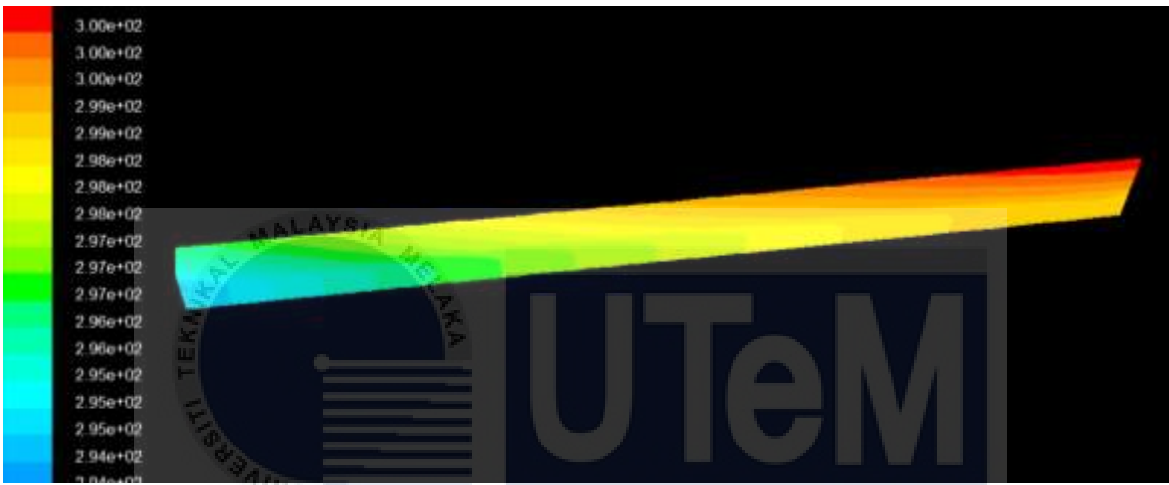


Figure 4.7: Local temperature distribution contour in the x-z plane
 (b) Sidewall plane for laminar flow

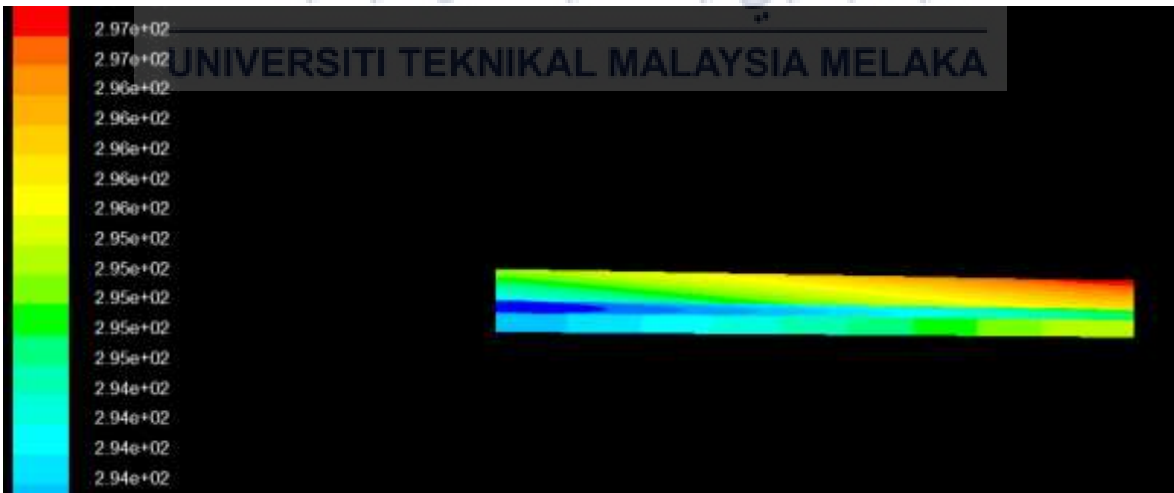


Figure 4.8: Local temperature distribution in the x-z plane
 (a) Middle plane for turbulent flow

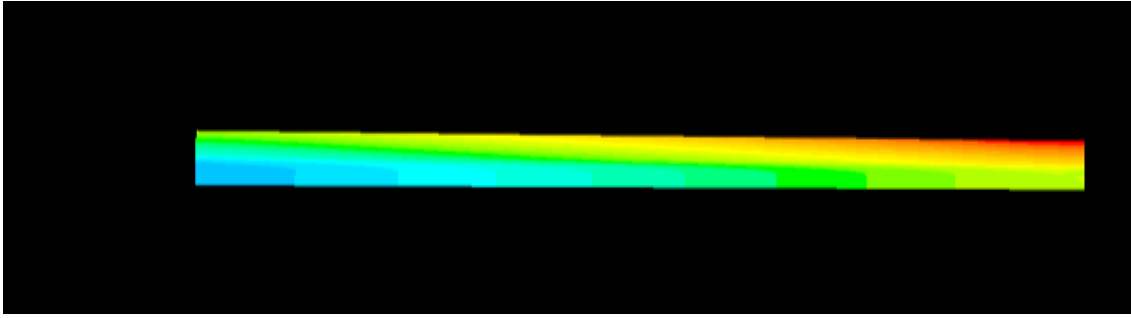
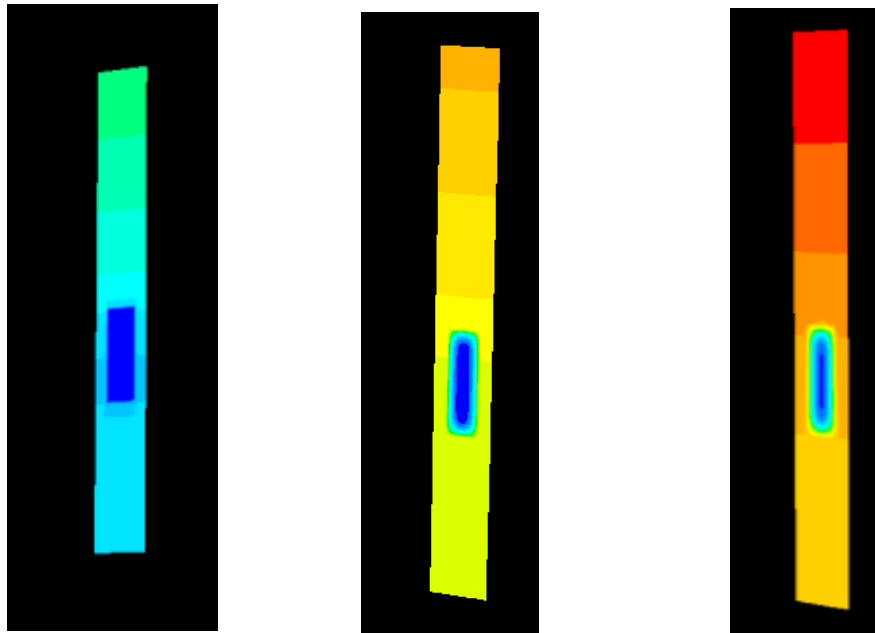


Figure 4.8: Local temperature distribution in the x-z plane

(b) Sidewall plane for turbulent flow

Figure 4.7(a) and Figure 4.7(b) show the temperature distribution at the x-z planes at the middle plane and side wall plane for the laminar flow. From the Figure 4.7(a), the shape channel from the inlet to outlet become clearly visible due to the higher temperature gradient difference between the fluid and solid. The temperature distribution contour show in Figure 4.7(a) and Figure 4.8(a), the temperature in laminar flow was much higher than turbulent flow in the middle and side wall. This is due to the laminar flow have higher heat flux. As the present of the heat flux, means there are more quantity of heat entering the fluid particles. The temperature distribution contour for the transfer of heat for heat sink inlet, heat sink middle and heat sink outlet for the $x=0$, $x=5$ and $x=10$ mm are showing in y-z plane. Figure 4.11(a), (b) and (c) are showing the contour of heat transfer for laminar flow in y-z plane while figure 4.12(a), (b) and (c) shows are shows the contour heat transfer for turbulent flow in y-z plane. Based on the Figure 4.11 and 4.12, the variation temperature for the liquid is much bigger than the solid. At the inlet $x = 0$ mm of the channel, the fluid temperature is uniform but due to the development of the thermal boundary layer, the temperature are changes. The temperature contour for laminar and turbulence are same and identically because thermal boundary layer do not occurs at this state. At the heat sink middle $x = 5$ mm and the heat sink outlet $x = 10$ mm, the thermal boundary layer have been occurs.

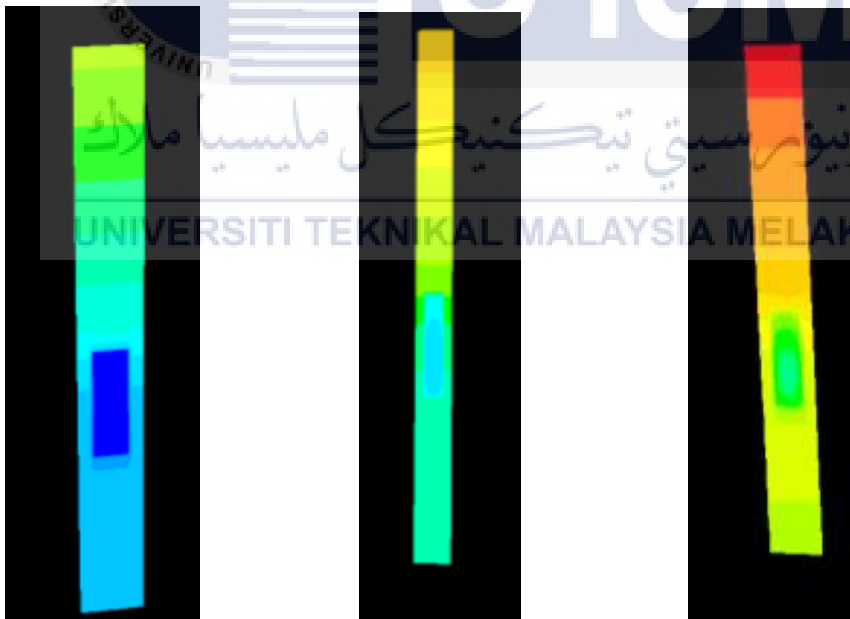


a) $x = 0$

b) $x = 5\text{mm}$

c) $x = 10\text{mm}$

Figure 4.9: Local temperature contours in y-z plane for laminar flow (a) heat sink inlet $x = 0$ mm (b) heat sink middle plane $x = 5$ mm (c) heat sink outlet $x = 10$ mm



a) $x = 0\text{mm}$

b) $x = 5\text{mm}$

c) 10mm

Figure 4.10: Local temperature contours in y-z plane for turbulent flow (a) heat sink inlet $x = 0$ mm (b) heat sink middle plane $x = 5$ mm (c) heat sink outlet $x = 10$ mm

4.5 Flow and Heat Transfer Analysis

Fully developed flow implies that the velocity profile does not change in the fluid flow direction hence the momentum also does not change in the flow direction. In such a case, the pressure in the flow direction will balance the shear stress near the wall. Flow and heat transfer investigation is to talk about the fully developed flow at the entrance region area for this microchannel. Hydrodynamic entrance region is refer to velocity profile which is the flow from the inlet point to the point where the velocity profile is fully developed. The hydrodynamic entrance region refers to the area of a region where fluid entering a region develops a velocity profile due to viscous forces propagating from the interior wall of a region. This region is characterized by a non-uniform flow. The fluid enters a region at a uniform velocity, then fluid particles in the layer in contact with the surface of the region come to a complete stop due to the no-slip condition. Due to viscous forces within the fluid, the layer in contact with the region surface resists the motion of adjacent layers and slows adjacent layers of fluid down gradually, forming a velocity profile.

4.5.1 Boundary Layer

Boundary layer region which is the region in which viscous effects and the velocity changes are significant. From the Figure 4.13 and Figure 4.14 below show the velocity profile in fully developed for laminar and turbulent. This all velocity profile are determined from rectangular microchannel heat sink hydrodynamic entrance length. Hydrodynamic entrance region is channel inlet to the point where the velocity profile fully developed. The length for that region is called hydrodynamic entry length. Hydrodynamic fully develop region is the region where the velocity profile fully developed and remain unchanged. There are different between laminar and turbulent velocity which is the turbulent flow is more flatter and fuller while laminar flow is parabolic

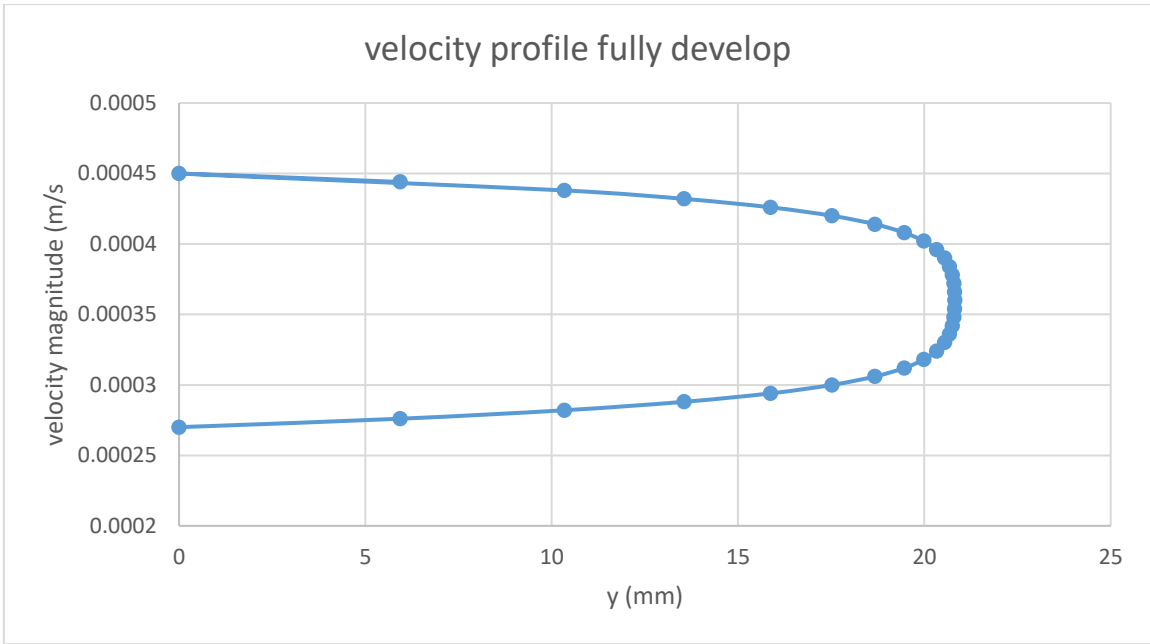


Figure 4.11: The velocity profile in fully developed for laminar flow

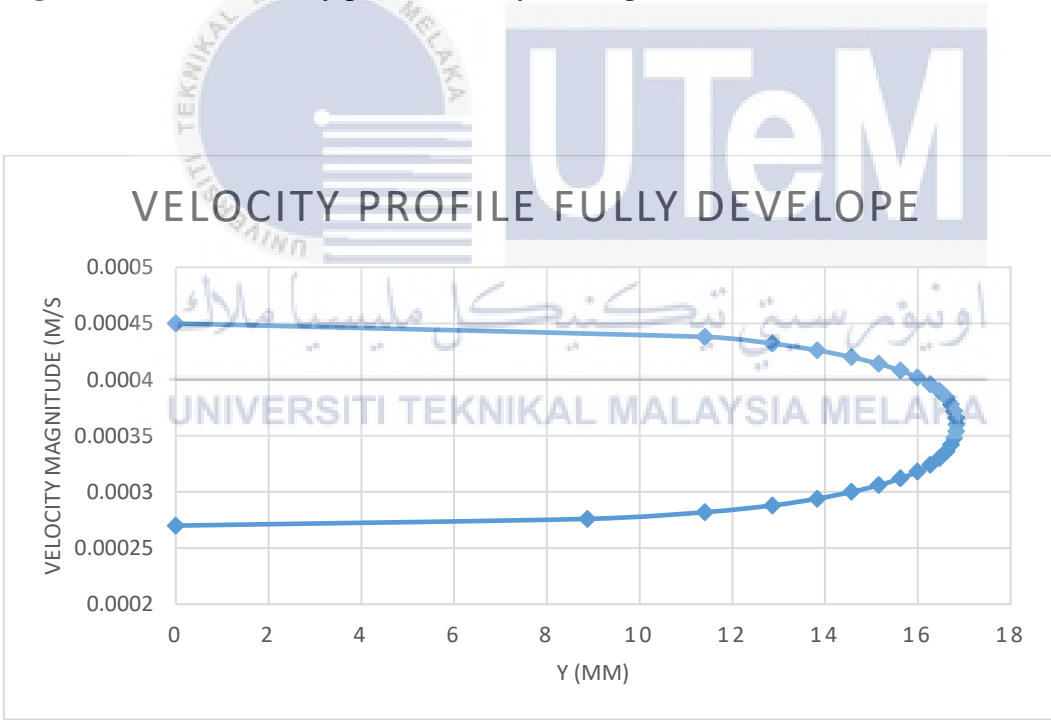


Figure 4.12: The velocity profile in fully developed for turbulent

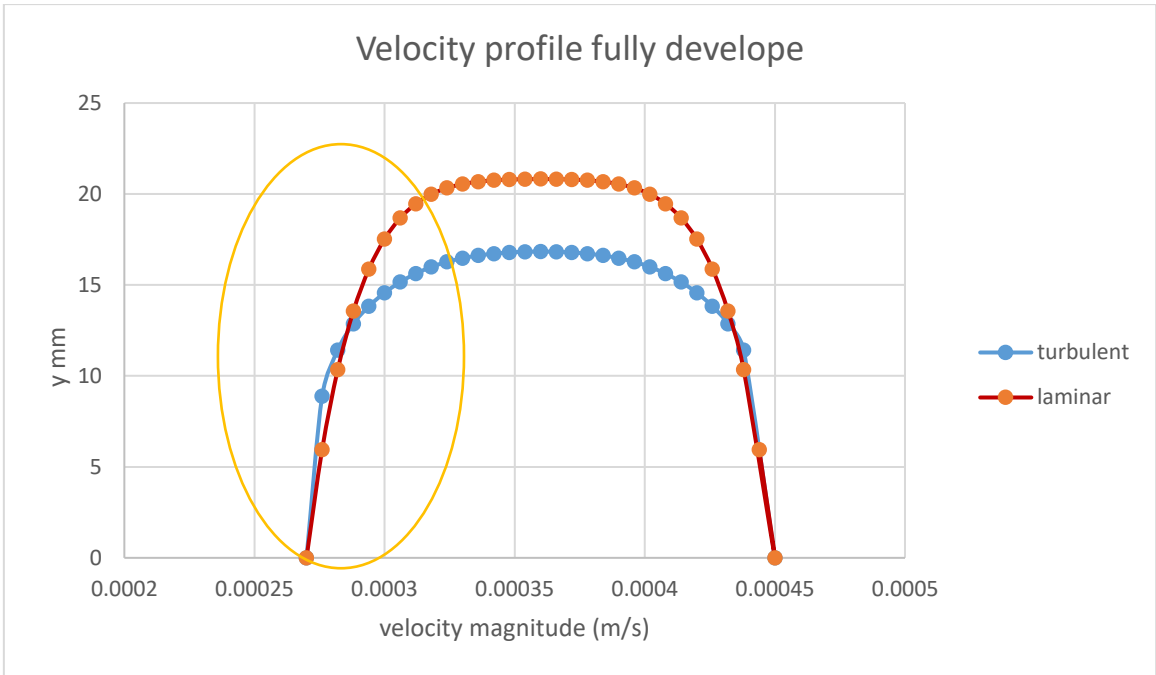


Figure 4.13: Shows the velocity profile in fully developed for laminar and turbulent flow

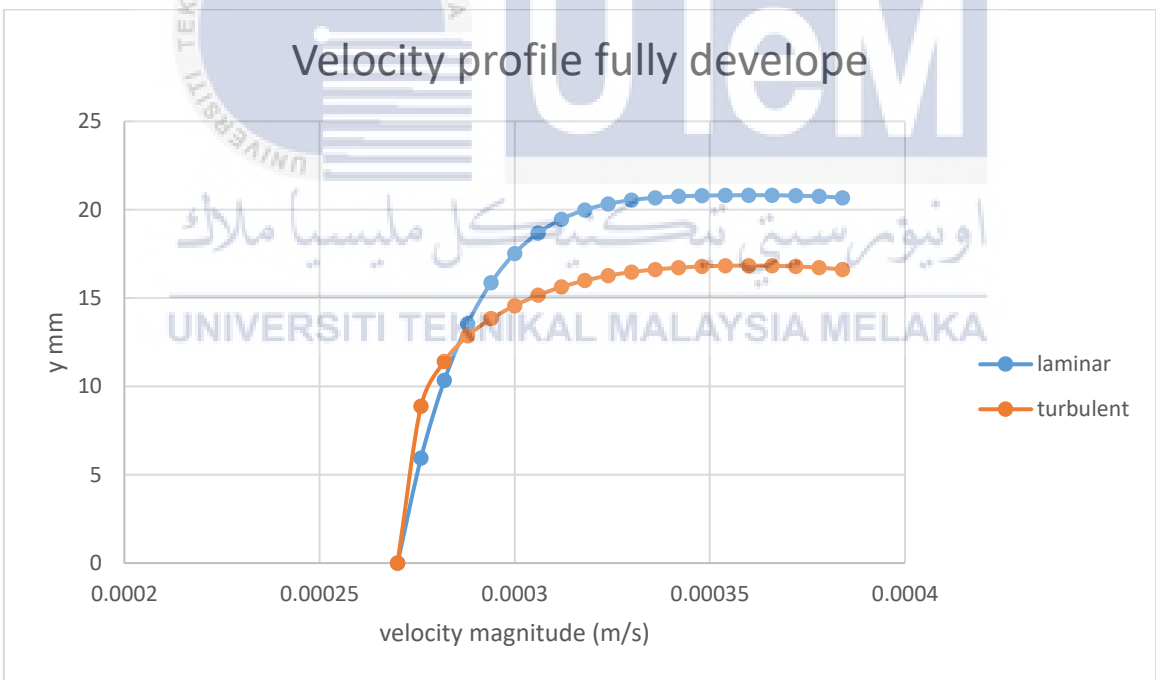


Figure 4.14: Shows the zooming velocity profile in fully developed for the laminar and turbulent flow

Figure 4.13 shows the velocity profile in fully developed for laminar and turbulent flow. The circle from Figure 4.13 is the area which is has been zooming in Figure 4.14. The main difference between laminar and turbulent flows lies in the complexity of flow patterns, which are far more complicated in turbulence due to seemingly random distribution of velocities in time, accompanied by large number of vortices of various sizes present all the time. When the flow is laminar, we have pressure forces being balanced by viscous forces, which are functions of mean velocity gradients and related through viscosity. In fully developed for laminar flow, all the particles of the water moves at constant axial velocity along the streamlines of the channel. Thus, velocity profile for laminar flow remains constants. There is no any motion in radial flow, thus we can assume all the velocity profile is zero along the normal directions. Since we assume the flow is steady, so there is no acceleration of the flow.

When the flow is turbulent, the effective shear force is not related to only mean velocity gradients but dominated by a much larger term known as the Reynolds stress, which in simple terms is related to square of the turbulent velocity fluctuations. Thus, deal with fully developed turbulent flows, the time averaged momentum equation has an additional term which plays the same role as an enhanced viscosity. This results in the velocity profile to be different from laminar flows. In fully developed for turbulence flow, swirling eddies in which the swirling motion caused by of positions and directions of turbulence flow. Swirling eddies will transport mass, momentum and energy that are more rapidly compare to the molecular diffusion and heat transfer that caused by the laminar flow. So, the friction values, heat transfer and mass transfer of turbulence flow are much higher compared to laminar flow.

4.6 Entrance length Laminar and Turbulent

In fluid dynamics, the entrance length is the distance a flow travels after entering a region before the flow becomes fully developed. Entrance length refers to the length of the entry region, the area following the regions entrance where effects originating from the interior wall of the regions propagate into the flow as an expanding boundary layer. When the boundary layer expands to fill the entire region, the developing flow become a fully developed flow, where flow characteristics no longer change with increased distance along the region. Many different entrance lengths exist to describe a variety of flow conditions. Hydrodynamic entrance length describes the formation of a velocity profile caused by viscous forces propagating from the region wall. Thermal entrance length describes the formation of a temperature profile.

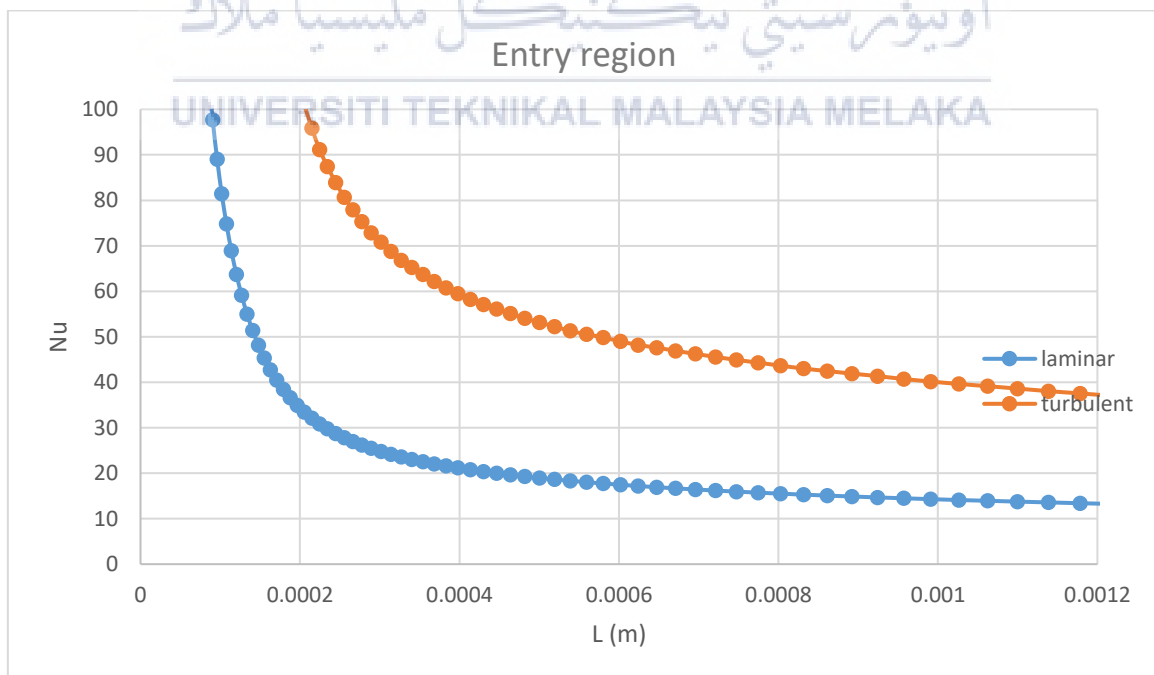


Figure 4.15: Entry length laminar and turbulent flow Nusselt number

Figure 4.15 shows the entry region for the laminar and turbulent at fully developed. This is obtain when the velocity profile remain constant along the channel. From that figure, length region for the laminar flow is much longer compare to the turbulence flow. This is due to the turbulence flow achieve fully developed faster and remain constant compared to the laminar.

4.6.1 Average Nusselt Number

In heat transfer at a boundary within a fluid, the Nusselt number (Nu) is the ratio of convective to conductive heat transfer across the boundary. In this context, convection includes both advection and diffusion. The conductive component is measured under the same conditions as the heat convection but with a hypothetically or motionless fluid. A similar non-dimensional parameter is biot number, with the difference that the thermal conductivity is of the solid body and not the fluid. This number gives an idea that how heat transfer rate in convection is related to the resulting of heat transfer rates in conduction. For example is a system consisting of a hot fluid getting heated which is in contact with a metal wall, a Nusselt number close to one namely convection and conduction of similar magnitude is characteristic of laminar flow. A larger Nusselt number corresponds to more active convection, with turbulent flow typically in the 100 to 1000 range. The convection and conduction heat flows are parallel to each other and to the surface normal of the boundary surface and are all perpendicular to the mean fluid flow in the simple case.

To investigate the effectiveness of the heat transfer from solid into the liquid of the design, the average Nusselt number is evaluated and plotted in Figure 4.14. The average

Nusselt number is calculated using equation (1) which is also included in journal Qu and Mudawar. To get the answer of the equation needs to find convective heat transfer first (H) which is the heat flux side wall need to divide with the value temperature side wall minus with temperature of middle wall. The value of H then insert to the equation of nusselt number which is need to times to D_h which is 4 times with area of design and divide with parameter of design. After times with D_h , devide with thermal conductivity of water which is 0.613 W/mk.

The effects of the solid thermal conductivity on the average Nusselt number are so small that the results for the copper heat sink are virtually identical. . Much higher average heat flux and Nusselt number can be found in the region near the channel inlet and decrease rapidly to nearly constant values. The average heat flux at the channel top wall is slightly larger than at the bottom wall, but the corresponding average Nusselt numbers are virtually identical. For most of the channel length, the average heat flux and Nusselt number at the channel top and bottom walls are about half their corresponding values at the channel side wall.

CHAPTER 5

CONCLUSION AND RECOMMENDATION

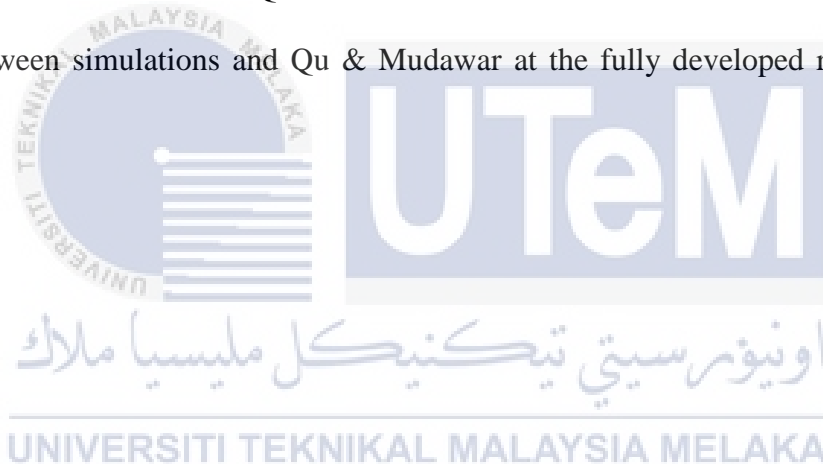
5.1 Introduction

In this chapter entitled Comparison of Laminar and Turbulent model of water Flow in Microchannel is performed by the simulations for water flow which is water through the rectangular copper microchannel by using the laminar and turbulent model. The result and discussion of numerical analysis will concluded and recommended. The thermal and hydrodynamic characteristics of microchannel are has been discussed. The fluid flow and heat transfer were analysed based on the simulations. The detailed of the average heat transfer such as temperature and Nusselt number was obtained. The entrance length was and velocity profile were obtained.

5.2 Conclusion

In the end, the average temperature distribution, the heat sink top wall has occur the higher temperature above the channel outlet compared to the heat sink bottom wall. The temperature rise along the flow direction in solid and fluid region can be approximately linear. The shape of the channel is clearly visible due to the large difference in temperature gradient between the solid and liquid. Because of the copper high thermal conductivity, the temperature gradient in the copper is much smaller than that in water.

Fully developed flow implies that the velocity profile does not change in the fluid flow direction hence the momentum also does not change in the flow direction. In such a case, the pressure in the flow direction will balance the shear stress near the wall. The main difference between laminar and turbulent flows lies in the complexity of flow patterns, which are far more complicated in turbulence due to seemingly random distribution of velocities in time. When the flow is laminar, we have pressure forces being balanced by viscous forces and when the flow is turbulent, the effective shear force is not related to only mean velocity gradients but dominated by a much larger term known as the Reynolds stress, which in simple terms is related to square of the turbulent velocity fluctuations. The largest deviation between simulation result from Qu and Mudawar result is 13.1%. The deviation of Nusselt number between simulations and Qu & Mudawar at the fully developed region is about 8.16%.



REFERENCE

Mudawar, Assessment of high-heat-flux thermal management Schemes, in: *Proceedings of the Seventh Intersociety Conference on Thermal and Thermomechanical Phenomena in Electronic Systems*, vol. 1, 2000, pp. 1–20.

Hiroaki Nishikawa, Yi Liu (Hiroaki Nishikawa & Yi Liu 2017) hyperbolic advection diffusion schemes for high Reynolds number boundary layer problems. *Journal of Computational Physics* 352 (2018) 23–51

Yong-Hui Wang, Ji-Li Zhang, Zhi-Xian Ma, 2017. Experimental study on single-phase flow in horizontal internal helically finned tubes the critical Reynolds number for turbulent flow. *Experimental Thermal and Fluid Science* 2017.11.003

Yunus A. Cengel, John M. Cimbala, 2014 *Fluid Mechanics, third edition in SI unit, printed in Singapore*, “The boundary layer approximation”, pp. 554-558.

L.T. Yeh, Review of heat transfer technologies in electronic Equipment, *ASME J. Electron. Package*. 117 (1995) 333–339.

D.B. Tuckerman, R.F.W. Pease, High-performance heat sinking for VLSI, *IEEE Electron. Dev. Lett.* EDL-2 (1981) 126–129.

Mudawar, M.B. Bowers, Ultra-high critical heat flux (CHF) for subcooled water flow boiling—I: *CHF data and parametric effects for small diameter tubes*, *Int. J. Heat Mass Transfer* 42 (1999) 1405–1428.

Z. Y. Guo, Z. X. Li, *Int. J. Heat Mass Transfer* **2003**, 46, 149-159. DOI: 10.1016/S0017-9310(02)00209-0

H.Y. Wu, and P. Cheng, *Int. J. Heat Mass Transfer* **2003**, 46, 2547-2556. DOI: 10.1016/S0017-9310(03)00035-8

A. Beskok, G.E. Karniadakis, Simulation of heat and momentum transfer in complex microgeometries, *J. Thermophys. Heat Transf.* 8 (4) (1994) 355e370
A. Beskok, G.E. Karniadakis, Simulation of heat and momentum transfer in complex micro-geometries, *J. Thermophys. Heat Transf.* 8 (4) (1994) 355e370

Zhu,Z.B., Tao,Z., Tian,Y.T., et al. [2016], Experimental Investigation of the Air Flow Behavior and Heat Transfer Characteristics in Microchannels with Different Channel Lengths, *ASME 2016 5thMicro/Nanoscale Heat and Mass Transfer International Conference, 3-6 January 2016 Biopolis, MNHMT2016-6612.*

C. Rands, B.W. Webb, D. Maynes (2005). Characterization of transition to turbulence in microchannel. *International Journal of Heat and Mass Transfer* 49 (2006) 2924–2930

K.V. Sharp, R.J. Adrian, Transition from laminar to turbulent flow in liquid filled micro tubes, *Exp. Fluids* 36 (2004) 741–747.

X.F. Peng, G.P. Peterson, B.X. Wang, Frictional flow characteristics of water flowing through rectangular microchannel, *Exp. Heat Transfer* 7 (1994) 249–264.

Gian Luca Morini (2010). Laminar to turbulent flow transition in microchannel. *International Journal of Heat and Mass Transfer.*

I. Mudawar, M.B. Bowers, Ultra-high critical heat flux (CHF) for subcooled water flow boiling I: CHF data and parametric effects for small diameter tubes, *Int. J. Heat Mass Transfer* 42 (1999) 1405–1428.

Weilin Qu, Issam Mudawar (2002), Analysis of three-dimensional heat transfer in microchannel heat sinks. *International Journal of Heat and Mass Transfer* 45 (2002) 3973–3985